NON-LINEAR SEISMIC RESPONSE OF BASE-ISOLATED FRAME STRUCTURES USING RUBBER BEARINGS

By
Iyad Munther S. Amareen

Supervisor
Prof. Abdelqader S. Najmi

Co-Supervisor
Dr. Anis S. Shatnawi

This Thesis was Submitted in Partial Fulfillment of the Requirements for the Master's Degree of Science in Civil Engineering

Faculty of Graduate Studies
The University of Jordan

August, 2007

This Thesis (Non-Linear Seismic Response of Base-Isolated Frame Structures Using Rubber Bearings) was successfully defended and approved on Thursday, August 2, 2007.

Examination Committee	Signature
Prof. Abdel-Qader S. Najmi Supervisor and Chairman Prof. of Civil Engineering	----------
Dr. Anis S. Shatnawi, Co-Supervisor Assist. Prof. of Civil Engineering	----------
Prof. Samih S. Qaqish, Member Prof. of Civil Engineering	----------
Prof. Yasser M. Hunaiti, Member Prof. of Civil Engineering	----------
Dr. Samir Z. Al-Sadder, Member Assist. Prof. of Civil Engineering Civil Engineering Company/Private Sector	----------

DEDICATION

To my beloved parents and brother

AKNOWLEDGEMENT

The author wishes to express his appreciation and gratitude to his supervisor Professor Abdelqader S. Najmi and to his co-supervisor Dr. Anis S. Shatnawi for their guidance and encouragement throughout the course of this program. Special thanks go to Dr. Shatnawi for his efforts in preparing this work. Thanks are also due to Professor Abdelqader S. Najmi, Prof. Samih S. Qaqish, Prof. Yasser Hunaiti and Dr. Samir AL-Sadder, for their service in the thesis advisory committee.

Finally, the author expresses special thanks to his parents for all the years of their sacrifices and encouragement.

Table of Content

Page

Committee Decision……...…ii

Dedication. ……iii

Acknowledgement……....iv

Table of Content……..……v

Notation……..vii

List of Tables……....ix

List of Figures ……..……..x

Abstract……..……..……..……...xiii

Chapter 1: Introduction ……..…1

1.1 Background and Research Significance……...……..…1

1.2 Previous Studies…...…...……..……...….3

1.3 Objectives of Research…..……....4

1.4 Research Methodology and Limitations……....5

Chapter 2: Literature Survey……..……7

2.1 Hyperelastic Model in Large Strain……..……7

2.2 Rubber-Steel Bearings……..……..……8

Chapter 3: Theory of Large Strain and Integration Algorithm……..10

3.1 Large Deformation Mechanics……10

3.2 Hyperelasticity ……14

3.3 Implicit Dynamic Analysis Using Direct Integration……...16

Page

Chapter 4: Description of the Structures and Modeling……..…….21

4.1 Overview……..….21

4.2 Description of the Rubber-Steel Bearings……24

4.3 Rubber Bearing Connection ……...…….36

4.3.1 Major Connection Types in ABAQUS Library……...….36

4.3.2 WELD Connection……....37

4.3.3 TIE Constraint……...38

4.4. Description of the Fixed-Base and Base-Isolated Steel Frame Structures……..39

4.4.1 Low-Rise Frame Model……. ……...….39

4.4.2 High-Rise Frame Model……...….39

Chapter 5: Results and Discussion ……..…42

5.1 Overview……..42

5.2 Rubber-Steel Bearing Models and Verification……...43

5.3 Low-Rise Frame Model……....49

5.4 High-Rise Frame Model…….. 57

Chapter 6: Conclusions and Recommendations……66

6.1 Conclusions……....66

6.2 Recommendations……...….67

References……68

Appendix A: Sample of ABAQUS Input Files 71

Abstract (ARABIC)……..75

Notation

a_n	Material constant
C_{ij}	Right Cauchy deformation tensor
$\hat{\mathbf{C}}$	Modified volumetric preserving deformation tensor
ds	Length for the final configuration
ds'	Length for the initial configuration
e^{α}	Orthonormal base vectors defining the axis system of the body
E_{ij}	Green-Lagrange strain tensor
F_{ij}	Deformation gradient tensor
$\hat{\mathbf{F}}$	Isochoric distortional deformation
f	Body force at a point
I	Second moment of area
I^N	Internal force vector
J	Jacobian
$L^N\big\|_{t+\Delta t}$	Sum of Lagrange multiplier forces associated with degree of freedom N
M^{NM}	Consistent mass matrix
N	Shape function
P^N	External force vector
u	Displacement
ü	Acceleration
$\ddot{u}^M$	Acceleration of the nodal variables
$\hat{W}$	Ogden strain energy function
x_i	Position vectors in the deformed configuration

X_i	Position vectors in the initial configuration
α	Artificial damping
α_n	Material constant
$\overline{\alpha}_p$	Material parameter
$\Delta\mathbf{C}$	Incremental rotation matrix
δ_{ij}	Kronecker delta
$\dot{\phi}$	Angular velocity
$\ddot{\phi}$	Angular acceleration
$\hat{\lambda}$	Principal values of $\hat{\mathbf{C}}$
μ_p	Material parameter
$\Delta\theta$	Increment in rotation
$\Delta\hat{\theta}$	Skew-symmetric matrix with axial vector $\Delta\theta$
ρ	Density

List of Tables

Table		Page
4.1	Material parameters of the rubber-steel bearings used to isolate the low-rise and high-rise frame models	28
4.2	Geometrical properties of the rubber-steel bearings used to isolate the low-rise and high-rise frame models	28
4.3	Uniaxial, Biaxial and Planar test data	31
4.4	Geometrical properties of the beams and columns of the low-rise frame model	41
4.5	Geometrical properties of the beams and columns of the high-rise frame model	41

List of Figures

Figure **Page**

1.1: Input ground acceleration of El-Centro, N-S earthquake……2

3.1: Relationship between the initial and deformed configurations of the body……...11

4.1: Fixed-base and base-isolated buildings……..23

4.2: Rubber-steel bearing used for isolating the low-rise frame model……26

4.3: Rubber-steel bearings used for isolating the high-rise frame model…….....27

4.4: Base-isolated low-rise steel frame model……..……30

4.5: Base-isolated high-rise steel frame model……...…...31

4.6: Tests performed for the rubber material provided by ABAQUS (a) Uniaxial test (b) Biaxial test (c) Planar test……..……...32

4.7: Nominal stress vs. nominal strain for a uniaxial test of rubber material……...….33

4.8: Nominal stress vs. nominal strain for a biaxial test of rubber material……..34

4.9: Shear stress vs. shear strain for a planar test of rubber material…….....……35

4.10: WELD connection in ABAQUS……..…….38

5.1: Stress in the x-direction versus the position from the left end at the bottom of the rubber-steel bearing…….…..45

5.2: Stress in the y-direction versus the position from the left end at the bottom of the rubber-steel bearing……...46

5.3: Horizontal acceleration versus time of a node located at the upper-right corner of the rubber-steel bearing……...47

5.4: Horizontal displacement versus time of a node located at the upper-right corner of the rubber-steel bearing……...48

5.5: Horizontal acceleration versus time for a node located at the upper-right corner of the fixed-base and base-isolated low-rise frame models……...…..51

Figure **Page**

5.6: Horizontal displacement versus time for a node located at the upper-right corner of the fixed-base and base-isolated low-rise frame models……...52

5.7: Relative displacement versus time of a node located at the upper-right corner of the fixed-base and base-isolated low-rise frame models……..53

5.8: The floor number versus the horizontal force for the fixed-base low-rise frame model……....54

5.9: The floor number versus the horizontal force for the base-isolated low-rise frame model……54

5.10: Lateral force versus the lateral displacement for a node located at the upper right corner of the fixed-base low-rise frame model……..55

5.11: Lateral force versus the lateral displacement for a node located at the upper-right corner of the base-isolated low-rise frame model……..55

5.12: Reaction force in the x-direction versus time for a node located at the lower-right corner of the fixed-base and base-isolated low-rise frame models…....56

5.13: Horizontal acceleration versus time for a node located at the upper-right corner of the fixed-base and base-isolated high-rise frame models……....59

5.14: Horizontal displacement versus time for a node located at the upper-right corner of the fixed-base and base-isolated high-rise frame models……..60

5.15: Relative displacement versus time of a node located at the upper-right corner of the fixed-base and base-isolated high-rise frame models……61

5.16: The floor number versus the horizontal force for the fixed-base high-rise frame model……...62

Figure **Page**

5.17: The floor number versus the horizontal force for the base-isolated high-rise frame model…….. 62

5.18: Lateral force versus the lateral displacement for a node located at the upper right corner of the fixed-base high-rise frame model……...63

5.19: Lateral force versus the lateral displacement for a node located at the upper-right corner of the base-isolated high-rise frame model…….63

5.20: Reaction force in the x-direction versus time for a node located at the lower-right corner of the fixed-base and base-isolated high-rise frame models..…64

Non-Linear Seismic Response of Base-Isolated Frame Structures Using Rubber Bearings

By
Iyad M. Amareen

Supervisor
Prof. Abdelqader S. Najmi

Co-Supervisor
Dr. Anis S. Shatnawi

ABSTRACT

Over the past two decades, much progress has been made in research and application of the base isolation of structures as means of providing earthquake resistance to a structure. However, the trade-off between the extent of acceleration reduction and the response of a base-isolation system has not been given a serious consideration. This work uses a new material constitutive model for rubber bearing base-isolation system, which adopts the technique of real-time structural parameter modification. To achieve this, a finite element modeling and analysis are performed as a comparative study between a conventional totally fixed-base steel framed structures and similar structures with base-isolation using rubber-steel bearings. The structures are subjected to the El-Centro, N-S earthquake.

In order to include nonlinearity effects, a non-linear hyperviscoelastic material model has been used and linked to ABAQUS software as a user defined material subroutine (i.e.; UMAT). Special connector elements are selected from ABAQUS library to connect the rubber bearings to the frame structure and the foundations in order to achieve the required kinematical constraints at the connection points.

The model is validated by carrying out a comparison study of the results obtained from the analysis of the presented material model with those obtained by using the existing ABAQUS material models (e.g., Ogden material model). The results show a significance efficiency of using the rubber bearing isolation in order to uncouple the structure from the seismic ground motion. Moreover, it has been proved that the used material model is more effective to capture the behavior of the base-isolated structures expressing a notable reduction in acceleration and increasing in the structural resistance to earthquake excitations.

Chapter One

INTRODUCTION

1.1 Background and Research Significance

Thousands of people died in different regions of the world because of the bad structural withstanding of earthquakes which led to structural collapses. Until recently, structures relied on their solidity and gravity mass in order to withstand external forces such as earthquakes. Nowadays, major advances have been achieved in earthquake-resistant design of structures and in the requirements of the building code related to this subject. Engineers tried to introduce and create some isolation systems using conventional materials such as steel and concrete. However, after introducing the uniform building code (UBC-97), isolation systems reached a new stage where high-technology structural elements were used side by side with the conventional materials creating a force-resisting system against earthquake excitation.

In order to uncouple structures from the seismic ground motion, special devices are inserted between the structure and its foundation such as the rubber-steel bearings to decrease the damage in the structure when subjected to a strong ground motion (Salomon O. et al., 1999). Rubber-steel bearing isolation is currently considered an effective technique for buildings protection in many countries because of the capability of the rubber bearings in sustaining large strains in shear and high loads in compression. This is due to the high horizontal flexibility and the high vertical stiffness in the rubber bearing isolation system. This study investigates the effect of inserting rubber-steel bearings to serve as a base isolation system between the structure and its foundation when the structure is subjected to El-Centro, N-S earthquake excitation (Figure 1.1).

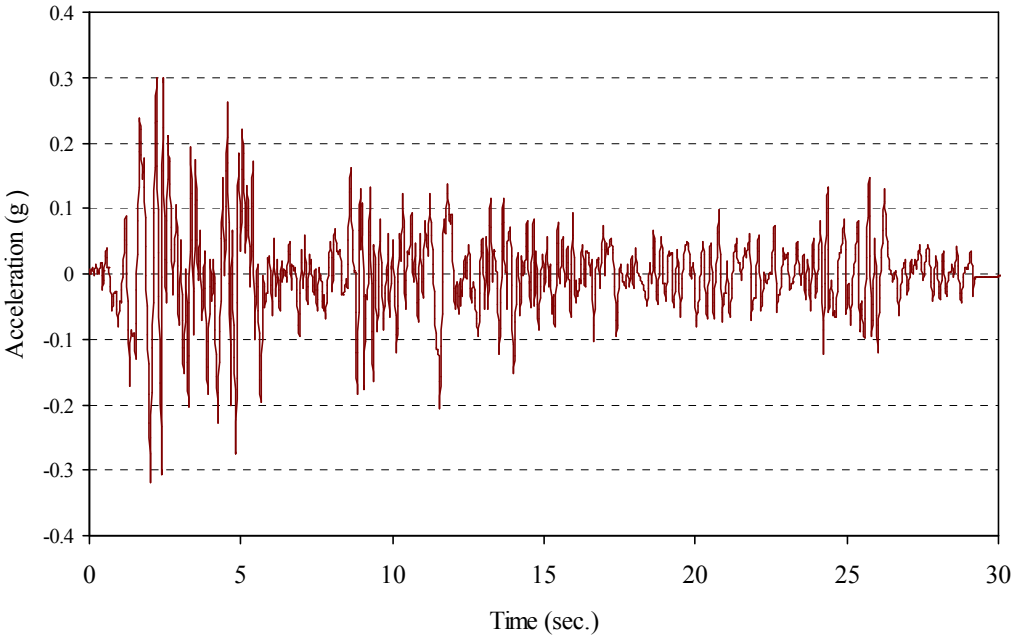

Figure 1.1: Input ground acceleration of El-Centro, N-S earthquake.

1.2 Previous Studies

Much research has been done in the past which investigated the seismic response of base-isolated single degree of freedom (SDOF) systems. These studies (Chopra A. K., 1995) treated the subject of base isolation systems in terms of the lead-rubber bearings which consist of a rubber layers reinforced with steel sheets and a lead core inserted in the middle in order to increase the vertical stiffness of the bearing when subjected to the seismic forces. These studies focused on the behavior of these types of isolation systems alone without coupling them with the real structures (Hwang J. S. et al., 2002). On the other hand, this study will be different because it emphasizes on using the rubber-steel bearing isolation system. Rubber-steel bearings consist of alternating layers of rubber and steel sheets without a lead core.

This study investigates the response of the isolation system and the behavior of the isolated structure together. Herein, the model created is for a structure connected to rubber-steel bearings isolation system using a suitable connection type, that is; WELD connection. The finite element model used for the rubber was created using the general software ABAQUS (Hibbitt, Karlsson and Sorensen, 2001).

Two strain energy potentials were used in material modeling of the rubber bearings. These are a proposed hyperviscoelastic material model found in Al-Shatnawi, 2001, which by default considers material time dependency, and the existing Ogden-type hyperelastic constitutive model found in ABAQUS. In order to validate the results obtained for the hyperelastic behavior of the rubber material, a comparison will be carried out between the ABAQUS results obtained for the rubber material and the results obtained from using a three-dimensional hyperviscoelasticity constitutive model for large strain that is implemented as a user-defined material subroutine in ABAQUS (i.e.; UMAT) (Al-Shatnawi A., 2001).

1.3 Objectives of Research

The main purpose of this study is to perform a non-linear seismic analysis for base-isolated frame structures using laminated rubber bearings. The focus will be on investigating the response of the base-isolated low-rise and high-rise steel structures along with the response of the rubber bearing system itself. The following detailed objectives are considered:

1. Introducing a non-linear elastic model for the rubber-steel bearing in order to investigate the non-linear seismic response of base-isolated buildings using rubber-steel bearings. However, the validity of this material model will be verified against the existing material models within the software ABAQUS.
2. To study the behavior of rubber-steel bearing and examine its functionality in elongating the period of the structure and decreasing the accelerations when the structure is subjected to an earthquake excitation. Hence; uncoupling the structure from the seismic ground motion.
3. To find the appropriate connector element that is capable of representing the kinematical constraints at the connection points between the rubber-steel bearings and the steel frames by employing it within the finite element model that is created using ABAQUS.
4. To investigate the non-linear seismic responses of base-isolated buildings using rubber-steel bearing system. Moreover, to carry out a comparative study of the seismic responses between the base-isolated and similar fixed-base frame structures to explore the effect of the rubber-steel bearings on the performance of buildings when subjected to earthquake excitation.

1.4 Research Methodology and Limitations

The seismic performance of base-isolated frame structures (using rubber-steel bearings) is investigated to be compared to similar fixed-base ones. Buildings with different floor levels and geometries will be examined.

The finite element models of the frame structures, rubber-steel bearings and one of the strain energy potentials that were used in modeling the rubber material were created using the general software ABAQUS. The software ABAQUS is a multi-purpose finite element program that can include nonlinearity such as the hyperelastic behavior of the rubber material.

In particular, this study includes the following steps:

1. A non-linear material constitutive model for large strain has been used and linked to the software ABAQUS as a user-defined material model subroutine (i.e.; UMAT) obtained from the study of Al-Shatnawi A., 2001. This model has been verified and checked against existing hyperelastic material models found within ABAQUS (e.g., Ogden model).
2. Assumptions when modeling hyperelastic material:
    - Nonlinear elastic behavior.
    - Isotropic material.
    - The simulation includes nonlinear material and geometric effects.
    - The analysis has been performed based on a two dimensional model.
3. The behavior of the rubber-steel bearings has been examined to ensure its functionality in elongating the period and decreasing accelerations of the structures when subjected to earthquake excitation.
4. Representative high-rise and low-rise steel frames (namely; four-story and fifteen- story), base isolated using rubber-steel bearings, are modeled using ABAQUS software.

5. A non-linear implicit dynamic seismic analysis is performed using direct integration method where the forcing function is given by the acceleration time history of the El-Centro, N-S earthquake. The responses are computed for the base-isolated and fixed-base structures to explore the effect of the rubber-steel bearings on the performance of the building.

   However, several complexities are involved in the analysis of base-isolated structures using rubber-steel bearings. These include:

   - Material nonlinearity:

     This source of nonlinearity is related to many factors such as strains, material failure and strain-rate-dependent material data. In the case of rubber-steel bearings, rubber is modeled as a nonlinear elastic material.

   - Geometric nonlinearity:

     This source of nonlinearity occurs when the magnitude of the displacements affects the response of the structure. This happens due to changes in the geometry of the model during the analysis. In the case of rubber-steel bearings, rubber undergoes large deformation that is greater than 5% strain (Al-Shatnawi A., 2001).

   - Choosing a connection element that is capable of modeling the connection between the structure and the rubber bearings in order to analyze the whole structure-base isolation system. In this case, a WELD connection is used to represent the actual practice of connection between the isolation system and the structural members. The results obtained are validated by comparing them with those obtained using the TIE constraint.

Chapter Two

LITERATURE SURVEY

2.1 Hyperelastic Model in Large Strain

Hyperelasticity is a constitutive model that is used to describe the non-linear elastic (large strain) materials responses. This model does not take memory effects or energy dissipation into account.

Important effects of material behavior were described phenomenologically by constitutive models in the past (Mooney, 1940, Rivlin, 1951, Ogden, 1984, Saleeb et al., 1992). An important development was due to Valanis and Landel, 1967, who separated the strain energy function into a separable form relating to the principal directions. This approach led to the Ogden model which is much used today (Ordonez D. et al., 2003).

Saleeb et al. (1992) had the ability to deal with the difficulty related to non-uniqueness of the principal values and associated eigenvectors and the fact of noncontinuity of their differentiable functions by developing an effective scheme to apply a class of Ogden-type hyperelastic constitutive models, for large strain analysis of rubber-like material. In later study, Gendy and Saleeb (2000) successfully implemented the derived hyperelastic model in a computational methodology to estimate the material parameters for characterizing general nonlinear material models for large strain analysis.

The literature mentioned above assumed a material behavior that does not depend on strain history. This is unlike the model used for describing the rubber behavior in the analysis of Al-Shatnawi (2001), where the hyperelastic numerical model takes viscoelasticity effect into account, i.e.; time dependent. This model adopted for the rubber deals with the continuum formulation of finite strain hyperviscoelasticity and provides its numerical simulation with a user's defined material subroutine (i.e.; UMAT)

in ABAQUS (Habbit, Karlsson, Sorensen, Inc., 1998). The material response is assumed to be modeled with a class of Ogden-type strain energy functions.

One of the rubber-steel bearing material models that are implemented in this study uses the strain energy potentials as found in ABAQUS, that is, the Ogden-type hyperelastic constitutive model used for large strain analysis of rubber materials. An experimental test data for the rubber material used in this study is taken from the ABAQUS manual (Habbit, Karlsson, Sorensen, Inc., 2001). The other material model for the rubber that is used in this study is that found in Al-Shatnawi, 2001. This material model takes into consideration the time dependency of the material behavior. It includes the viscoelasticity effects on the material behavior. This hyperviscoelastic material model is confirmed by comparing the results with those obtained using Ogden material model found in ABAQUS/STANDARD.

2.2 Rubber-Steel Bearings

Historically, major earthquakes caused damage to civil engineering structures in different regions of the world (Yefim G., 1999). The non-linear response of structures subjected to earthquake excitations has been a vital issue that worries engineers and researchers.

A lot of research work was reported on the subject of seismic behavior of base-isolated frame structures. However, few of these publications developed a model to describe the behavior of rubber bearings subjected to earthquake excitation or cyclic loading tests (Hwang J. S., 2002) and a fewer researches reported case studies of structures isolated using rubber bearings (Salomon O., 1999).

Hwang J. S. et al., 2002, presented a mathematical hysteretic model for elastomeric isolation bearings that was validated by material tests and the shaking table test. The model was capable of predicting the shear force-displacement hysteresis very

accurately for both rubber material and bearing under cyclic loading reversals. In other words, the model was capable of predicting the behavior of rubber material and the bearings when it experiences a dynamic shear loading. However, the proposed study did not introduce a case study of a structure isolated using the elastomeric isolation bearings.

Salomon O. et al., 1999, introduced an analytical and numerical model for a high damping rubber bearing that took into account the highly nonlinear elastic behavior of the rubber bearing and its energy dissipation. The Ogden strain energy function was used in the analysis. Also, the model was confirmed by comparing with existing experimental results. The results were much close. Also, in order to validate the rubber bearings model, the results for a base-isolated reinforced concrete frame, isolated using the rubber-bearings subjected to the El Centro earthquake was compared with a similar fixed-base structure. What was found is that the base-isolated structure has a much less acceleration at the top floor, inter-storey displacement and total structural displacement.

Few years later, Lee G. presented a case study on the effect of inserting high damping rubber bearings as a base isolation system to a symmetrical, low-rise reinforced concrete structure in Algeria. Lee G. designed two frames; a moment resisting and a base isolated frame. He found that although base isolators are expensive, they reduce the acceleration effectively. Also, they reduce the quantity of steel needed in design significantly (the moment resisting frame needs 3.3 times more steel as required in the base isolation frame). Also, Ordonez D, et al., 2003, presented a comparative study of the inelastic response of base isolated buildings. A nonlinear response spectrum for various design parameters was obtained using six earthquake records. One of the conclusions reached in this study is that the isolators affect significantly the structural response of old weak building systems.

Chapter Three

THEORY OF LARGE STRAIN AND INTEGRATION ALGORITHM

3.1 Large Deformation Mechanics

Large deformation is typically defined as a response having greater than 3 to 5% strain. This type of deformation must be treated using appropriate stress and strain tensors side by side with the appropriate constitutive relations. The rubber material used in the rubber-steel bearings allows both small and large deformations and shows nonlinear stress-strain dependence for finite deformations.

In order to define large deformation strain measure, the relationship between the initial and deformed configurations of the body (Figure 3.1) must be defined by vector addition as follows:

$$x_i = X_i + u_i \tag{3.1.1}$$

Where x_i and X_i are the position vectors in the initial and deformed configurations respectively while u_i is the displacement.

The derivation of equation (3.1.1) with respect to X leads to

$$\frac{\partial x_i}{\partial X_j} = \frac{\partial X_i}{\partial X_j} + \frac{\partial u_i}{\partial X_j} \tag{3.1.2}$$

Where $\frac{\partial X_i}{\partial X_j}$ is a second order identity tensor. It can be represented by the kronecker delta as:

$$\frac{\partial X_i}{\partial X_j} = \delta_{ij} \tag{3.1.3}$$

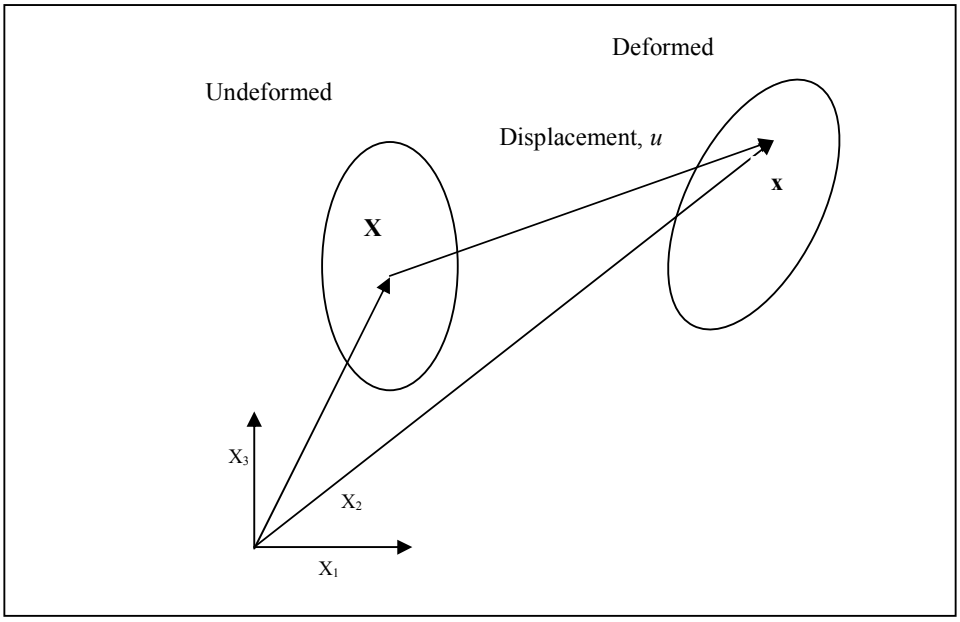

Figure 3.1: Relationship between the initial and deformed configurations of the body.

The material orientation vectors must also be defined in both initial and deformed configurations by using the finite element method mapping technique using the chain rule in equation (3.1.1) as follows

$$dx_i = \frac{\partial x_i}{\partial X_j} \partial X_J \tag{3.1.4}$$

$\frac{\partial x_i}{\partial X_j}$ is defined as the deformation gradient tensor and can be written as:

$$F_{ij} = \frac{\partial x_i}{\partial X_j} \tag{3.1.5}$$

Equation (3.1.2) can be rewritten by substituting equations (3.1.3) and (3.1.5) so it becomes:

$$F_{ij} = \delta_{ij} + \frac{\partial u_i}{\partial X_j} \tag{3.1.6}$$

F_{ij} is a second order tensor with the following three invariants :

$$I_1 = trF = F_{ij}\partial_{ij} = F_{11} + F_{22} + F_{33} \tag{3.1.7.a}$$

$$I_2 = \frac{1}{2}\left(F_{ij}F_{ij} - F_{ii}F_{jj}\right) \tag{3.1.7.b}$$

$$I_3 = \det \mathbf{F} = J \tag{3.1.7.c}$$

Where J is the deformation Jacobian.

In order to define a strain measure that is independent of the rigid body motion and rotation, the change in length squared in a material vector when going from the initial configuration to the deformed one must be measured.

The length squared could be written for the initial configuration as:

$$(ds')^2 = dX_i dX_i \tag{3.1.8}$$

For the final configuration:

$$(ds)^2 = dx_i dx_i \tag{3.1.9}$$

$$(ds')^2 - (ds)^2 = dX_i dX_i - dx_i dx_i = 2dX_i E_{ij} dX_j \tag{3.1.10}$$

Where E_{ij} is the strain tensor

Replacing dX by the deformation gradient tensor definition will reform the above equation into the following shape:

$$dx_i F_{ki} F_{kj} dx_j - dx_i dx_i = 2dX_i E_{ij} dX_j \tag{3.1.11}$$

Note that the following holds:

$$\underbrace{dx_i F_{ki}}_{dX_k} \underbrace{F_{kj} dx_i}_{dX_k} = dX_i dX_i = dX_i \delta_{ij} dX_j \tag{3.1.12}$$

Replacing k in the above equation with an i is acceptable since it is repeated in the equation:

$$dX_i dX_i = dX_i \delta_{ij} dX_j \tag{3.1.13}$$

Substituting the second and third terms of equation (3.1.12) in the strain equation, it becomes:

$$dX_i F_{ki} F_{kj} dX_j - dX_i \delta_{ij} dX_j = dX_i \left(F_{ki} F_{kj} - \delta_{ij}\right) dX_j = 2dX_i E_{ij} dX_j \tag{3.1.14}$$

From which the strain **E** could be written in terms of the deformation gradient tensor as:

$$E_{ij} = \frac{1}{2}\left(F_{ki} F_{kj} - \delta_{ij}\right) \tag{3.1.15}$$

The right Cauchy deformation tensor, C_{ij}, is defined as:

$$\mathbf{C} = \mathbf{F}^{\mathrm{T}} \mathbf{F} \tag{3.1.16a}$$

Or, in another form:

$$C_{ij} = F_{ki} F_{kj} \tag{3.1.16b}$$

Using the right Cauchy deformation tensor, the Green-Lagrange strain tensor can be rewritten as:

$$E_{ij} = \frac{1}{2}(C_{ij} - \delta_{ij}) \tag{3.1.17}$$

The equations above are used in creating the hyperviscoelastic model in the study of Al-Shatnawi, 2001, that is implemented as a user-defined material subroutine (UMAT) in ABAQUS. In order to validate the results obtained from using this model of large strain behavior, a comparison is carried out with using the hyperelastic rubber material, found in ABAQUS for the rubber material.

3.2 Hyperelasticity

Next stage is to consider the hyperelastic behavior of the rubber material used in the rubber bearings. Hyperelasticity is a type of material behavior that includes the nonlinear elastic response of some kinds of materials with large strains. It is a time independent nonlinear phenomena that takes energy dissipation into account. In other words, the behavior of a hyperelastic isotropic material case is studied by describing the material using strain energy potential. Due to incompressibility of the rubber material, an uncoupled volumetric/deviatoric form of strain energy is considered (Al-Shatnawi A., 2001).

Decomposing the gradient deformation tensor, **F**, the right Cauchy tensor, **C** and the Langrangian strain tensor, **E** will result with the following equations:

$$\mathbf{F} = J^{1/3}\,\hat{\mathbf{F}} \tag{3.2.1a}$$

$$\hat{\mathbf{C}} = J^{-2/3}\,\mathbf{C} = \hat{\mathbf{F}}^{\mathrm{T}}\hat{\mathbf{F}} \tag{3.2.1b}$$

$$\hat{\mathbf{E}} = \frac{1}{2}\left(\hat{\mathbf{C}} - \mathbf{I}\right) \tag{3.2.1c}$$

Where $\hat{\mathbf{F}}$ is the isochoric distortional deformation ($\det \hat{\mathbf{F}} = 1$), $J^{1/3}\mathbf{I}$ is the pure dilatation and $\hat{\mathbf{C}}$ is the modified, volumetric preserving deformation tensor (Saleeb et al., 1992 and Hughes, 1998).

The directional derivative of $\hat{\mathbf{C}}$ is:

$$D\hat{\mathbf{C}} \bullet \mathbf{A} = J^{-2/3}\left[\mathbf{A} - \frac{1}{3}\left(\mathbf{C}^{-1} : \mathbf{A}\right)\mathbf{C}\right] \tag{3.2.2}$$

Where "**:**" means scalar multiplication (i.e.; trace operation).

Considering the variation of **A** in tensor **C**:

$$\frac{\partial \hat{\mathbf{C}}}{\partial \mathbf{C}} = J^{-2/3}\left[\mathbf{I}^{(4)} - \frac{1}{3}\mathbf{C} \otimes \mathbf{C}^{-1}\right] \tag{3.2.3}$$

where

"$\otimes$" is the vector product of tensors.

$\mathbf{I}^{(4)}$ is the unit tensor

$$I^{(4)}_{ijkl} = \frac{1}{2}\left(\delta_{ik}\delta_{jl} + \delta_{il}\delta_{jk}\right) \tag{3.3.4}$$

Next is representing the hyperelastic material by a strain energy function where Ogden model is adopted. The deviatoric part of the stored-energy function can be defined as:

$$\hat{W} \equiv \hat{W}\left(\hat{\lambda}_i\right) = \sum_{n=1}^{N} \frac{a_n}{\alpha_n}\left(\hat{\lambda}_1^{\alpha_n} \hat{\lambda}_2^{\alpha_n} + \hat{\lambda}_3^{\alpha_n} - 3\right) \tag{3.2.5}$$

where

$\hat{\lambda}$ are the principal values of $\hat{\mathbf{C}}$.

a_n and α_n are material constants.

In ABAQUS, the strain energy function representing the Ogden model of the material is represented by the following equation:

$$W = \sum_{p=1}^{N} \frac{2\mu_p}{\overline{\alpha}_p^2} \left(\lambda_1^{\overline{\alpha}_p/2} + \lambda_2^{\overline{\alpha}_p/2} + \lambda_3^{\overline{\alpha}_p/3} - 3 \right) \tag{3.2.6}$$

Where μ_p and $\overline{\alpha}_p$ are material parameters. They can be related to the material parameters a_n and α_n in equation (3.2.5) as follows:

$$\mu_p = 2\alpha_n a_n, \qquad \overline{\alpha}_p = 2\alpha_n \tag{3.2.7}$$

3.3 Implicit Dynamic Analysis Using Direct Integration

In order to study the dynamic response of the models adopted in this study, a suitable analysis method is chosen. Since nonlinearity is included in this analysis due to the large deformation in the rubber-steel bearings, a general dynamic analysis is chosen along with using a direct-integration dynamic analysis. To calculate the transient dynamic response of the system, implicit time integration is used.

Hilber-Hughes-Taylor operator which is an implicit method extended from the trapezoidal rule is the general direct integration method used by ABAQUS to perform the analysis. This is done by solving a set of simultaneous equations iteratively using Newton's method.

In studying structural systems, an unconditionally stable integration operator is more preferred than a conditionally stable integration operator because it is a less computationally expensive analysis. The Hilber-Hughes-Taylor operator is unconditionally stable for linear systems. For practical purposes, the linear stability results give a good indication of the integration method's properties for nonlinear systems.

The dynamic procedure assumes that the body force at a point, **f**, is written in terms of the body force and the d'Alembert force as:

f = **F**- d'Alembert force (3.3.1a)

or

$$\mathbf{f} = \mathbf{F} - \rho\,\ddot{\mathbf{u}} \tag{3.3.1b}$$

Where

f: Body force at a point

F: Externally prescribed body force

ρ: Current density of the material at the point

u: Displacement

$\ddot{\mathbf{u}}$: Acceleration

Or in terms of the of the virtual work equation

$$\int_V \mathbf{f}.\delta\mathbf{v}\ dV = \int_V \mathbf{F}.\delta\mathbf{v}\ dV - \int_V \rho\,\ddot{\mathbf{u}}.\delta\mathbf{v}\ dV \tag{3.3.2}$$

If reference volume and reference density are used in the d'Alembert force term, then, it will be written as

$$\int \rho_\circ \ddot{\mathbf{u}}\,.\,\delta\mathbf{v}\ dV_\circ \tag{3.3.3}$$

The interpolator approximates the displacement at a point as

$$\mathbf{u} = \mathbf{N}^{\mathbf{N}}\ u^N \tag{3.3.4}$$

Consequently

$$\ddot{\mathbf{u}} = \mathbf{N}^{\mathbf{N}}\ \ddot{u}^N \tag{3.3.5}$$

Where

$\mathbf{N}^{\mathbf{N}}$ is the shape function for node N and it is not displacement dependent

By substituting the interpolations in the d'Alembert force term, it becomes

$$-\left(\int_{V_\circ} \rho_\circ \mathbf{N}^{\mathbf{N}} \cdot \mathbf{N}^{\mathbf{M}}\ dV_\circ\right)\ddot{u}^M \tag{3.3.6}$$

In the above equation, the integration between brackets is called the consistent mass matrix while $\ddot{u}^M$ is the acceleration of the nodal variables.

Thus, the equilibrium equation can be rewritten using the finite element approximation as follows:

$$M^{NM}\ddot{u}^{M} + I^{N} - P^{N} = 0 \tag{3.3.7}$$

Note that

$$M^{NM} = \int_{V_\circ} \rho_\circ \mathbf{N^N} \cdot \mathbf{N^M}\, dV_\circ \tag{3.3.8a}$$

M^{NM} : Consistent mass matrix

$$I^{N} = \int_{V_\circ} \beta^{N} : \boldsymbol{\sigma}\, dV_\circ \tag{2.4.8b}$$

I^{N} : Internal force vector

$$P^{N} = \int_{S} \mathbf{N^N}.\ \mathbf{t}\ dS + \int_{V} \mathbf{N^N} \cdot \mathbf{F}\ dV \tag{3.3.8c}$$

P^{N} : External force vector

The implicit operator defined by Hilber and Hughes is used for time integration of the dynamic problem. It replaces the equilibrium equation with the following equation:

$$\begin{aligned} M^{NM}\ddot{u}^{M}\big|_{t+\Delta t} + (1+\alpha)(I^{N}\big|_{t+\Delta t} \\ - P^{N}\big|_{t+\Delta t}) - \alpha(I^{N}\big|_{t} - P^{N}\big|_{t}) + L^{N}\big|_{t+\Delta t} = 0 \end{aligned} \tag{3.3.9}$$

Where $L^{N}\big|_{t+\Delta t}$ is the sum of all Lagrange multiplier forces associated with degree of freedom *N*.

The operator definition is completed by the Newmark formulae for displacement and velocity integration:

$$\mathbf{u}\big|_{t+\Delta t} = \mathbf{u}\big|_{t} + \Delta t\, \dot{\mathbf{u}}\big|_{t} + \Delta t^{2}\left(\left(\frac{1}{2} - \beta\right)\ddot{\mathbf{u}}\big|_{t} + \beta\, \ddot{\mathbf{u}}\big|_{t+\Delta t}\right) \tag{3.3.10}$$

And

$$\dot{\mathbf{u}}\big|_{t+\Delta t} = \dot{\mathbf{u}}\big|_{t} + \Delta t\left((1-\gamma)\ddot{\mathbf{u}}\big|_{t} + \gamma\, \ddot{\mathbf{u}}\big|_{t+\Delta t}\right) \tag{3.3.11}$$

Where

$$\beta=\frac{1}{4}(1-\alpha)^2,\quad \gamma=\frac{1}{2}-\alpha \quad \text{and} \quad -\frac{1}{3}\le\alpha\le 0 \tag{3.3.12}$$

Damping is considered here using the artificial damping. Artificial damping is controlled through the numerical damping control parameter; α. This damping control parameter ranges from 0 to -1/3. When α equals to "0" means that there is no artificial damping while $\alpha = -1/3$ provides the maximum artificial damping which gives about 6% damping ratio when the period of oscillation is 2.5 times the time increment.

The accelerations are integrated in the body axis system, so that Newmark's formula gives the change in velocity as

$$\dot{\phi}^{\alpha}\big|_{t+\Delta t}=\dot{\phi}^{\alpha}\big|_{t}+\Delta t[\gamma\ddot{\phi}^{\alpha}\big|_{t+\Delta t}+(1-\gamma)\ddot{\phi}^{\alpha}\big|_{t}] \tag{3.3.13}$$

Where $\dot{\phi}^{\alpha}$ and $\ddot{\phi}^{\alpha}$ are the angular velocity and the angular acceleration

If the global system is considered the above equation will be:

$$\dot{\phi}\big|_{t+\Delta t}=\Delta t\gamma\ddot{\phi}\big|_{t+\Delta t}+[e^{\alpha}\big|_{t+\Delta t}+e^{\alpha}\big|_{t}][\dot{\phi}\big|_{t}+\Delta t(1-\gamma)\ddot{\phi}\big|_{t}] \tag{3.3.14}$$

Where $e^{\alpha}=e^{\alpha}(\phi)$ are the orthonormal base vectors defining the axis system of the body. Consequently, equation (3.3.14) could be rewritten as follows:

$$\dot{\phi}\big|_{t+\Delta t}=\Delta t\gamma\ddot{\phi}\big|_{t+\Delta t}+\Delta\mathbf{C}\,.[\dot{\phi}\big|_{t}+\Delta t(1-\gamma)\ddot{\phi}\big|_{t}] \tag{3.3.15}$$

$\Delta\mathbf{C}$ is the incremental rotation matrix

$$\Delta C=e^{[\Delta\hat{\theta}]} \tag{3.3.16}$$

Where $\Delta\theta$ is the increment in rotation while $\Delta\hat{\theta}$ is the skew-symmetric matrix with axial vector $\Delta\theta$.

Newmark's formula for the time integration of the rotation increment is:

$$\Delta\theta^{\alpha}=\Delta t\dot{\phi}^{\alpha}\big|_{t}+\Delta t^2[(\frac{1}{2}-\beta)\ddot{\phi}^{\alpha}\big|_{t}+\beta\ddot{\phi}^{\alpha}\big|_{t+\Delta t}] \tag{3.3.17}$$

After solving for the unknown velocity, the velocity equation will be:

$$\dot{\phi}\,\big|_{t+\Delta t} = \frac{\gamma}{\Delta t\beta}\Delta\theta + \Delta\mathbf{C}\,.[(1-\frac{\gamma}{\beta})\dot{\phi}\big|_t + \Delta t(1-\frac{\gamma}{2\beta})\ddot{\phi}\big|_t] \tag{3.3.18}$$

Consequently, the acceleration equation becomes:

$$\ddot{\phi}\big|_{t+\Delta t} = \frac{1}{\Delta t\gamma}\dot{\phi}\big|_{t+\Delta t} + \Delta\mathbf{C}\,.[(1-\frac{1}{\gamma})\ddot{\phi}\big|_t - \frac{1}{\Delta t\gamma}\dot{\phi}\big|_t] \tag{3.3.19}$$

Implicit dynamic analysis is expensive especially in time and hard work. However, it is one of the most suitable methods in dealing with nonlinear dynamic problems, in which, nonlinearity in material and geometry needs a large amount of work to deal with. Other conventional methods can not deal with such complicated cases. This gives a big credit to this method when it is compared to other methods.

Chapter Four

DESCRIPTION OF THE STRUCTURES AND MODELING

4.1 Overview

The conventional approach to earthquake resistant design of buildings depends upon providing the building with strength, stiffness and inelastic deformation capacity which are adequate to withstand a given level of earthquake generated force. This is generally accomplished through the selection of an appropriate structural configuration and the careful detailing of structural members, such as beams and columns, and the connection between them.

In addition to the above, the basic approach underlying more advanced techniques for earthquake resistance is not to strengthen the building, but to reduce the earthquake-generated forces acting upon it. Among the most important advanced techniques of earthquake resistant design and construction are base isolation and energy dissipation devices. The most widely used of these advanced techniques, is known as base isolation.

A base-isolated structure is supported by a series of bearings which are placed between the bottom of the building's columns and above its foundation as seen in Figure (4.1). A variety of different types of base isolation bearings have been developed. Among these are the rubber-steel bearings that are the most frequently-used types of base-isolation bearings. A rubber-steel bearing is made of layers sandwiched together with layers of steel. On the top and the bottom, the bearing is fitted (welded) with the steel plates which are used to attach the bearing to the building foundation. The bearing is very stiff and strong in the vertical direction, but flexible in the horizontal direction.

To get a basic idea of how base isolation works, one should examine the behavior of a base-isolated building against a conventional, fixed-base, building. Because of the

complex nature of earthquake ground motion, the building actually may tend to vibrate back and forth in varying directions. So, it is important to realize that buildings do not shift in only one direction, but it is really a kind of "snapshot" of the building at only one particular point of its earthquake response that may be taken into consideration.

To understand the response of a building when subjected to earthquake motion, one should realize the displacing of the building back and forth due to the excitation and the inertial forces that are proportional to the building acceleration during ground motion. The fixed-base building is shown to be changing its shape due to the building deformation. That is the main cause of damage to buildings.

By contrast, even though it is displacing too, the base-isolated building retains its original, rectangular shape while displacing. It is the rubber-steel bearing that deforms. The base isolated building itself escapes the deformation and damage which implies that the inertial forces acting on the base-isolated building have been reduced. This is due to the reduction in the acceleration of the building. Acceleration decreases because of the base-isolation system contribution in lengthening the building's period of vibration.

Finally, since they are highly elastic, the rubber-steel bearings do not suffer any damage. But the rubber sheets reduce or dissipate the kinetic energy of motion by converting it into heat. And by reducing the input energy to the building, it helps to slow and eventually stop the building's vibration sooner than the case of the fixed-base building. In other words, it damps the building vibration.

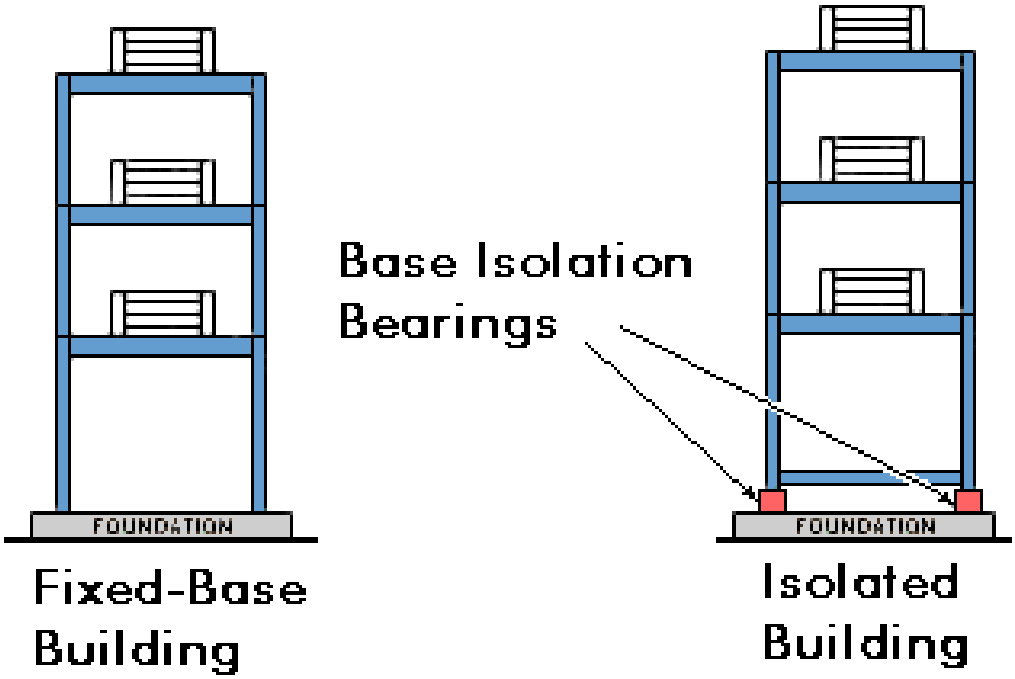

Figure 4.1: Fixed-base and base-isolated buildings.

4.2 Description of the Rubber-Steel Bearings

Rubber-steel bearings used in this study consist of alternating layers of rubber and steel. Rubber layers provide the required horizontal flexibility. While on the other side, the steel layers increase the vertical stiffness of the rubber bearings by reducing the bulging of the rubber.

Two models of the rubber-steel bearings with different dimensions were used in this study as shown in Figures (4.2) and (4.3). One is for the low-rise frame that is shown in Figure (4.4) and the other is for the high-rise frame shown in Figure (4.5). The material parameters of the rubber-steel bearings that are used to isolate the low-rise and high-rise frame models are listed in Table (4.1). On the other hand, the geometrical properties of the rubber-steel bearings that are used to isolate the low-rise and high-rise frame models are listed in Table (4.2). The meshes that were created for the rubber bearing models were chosen to be very fine meshes as it is seen in Figures (4.2) and (4.3). This helps in obtaining more accurate results and better convergence of the solution.

The model used for the rubber is created using ABAQUS and the strain energy potential that is used is the Ogden-type one-term (N=1) hyperelastic constitutive model. In order to define the hyperelastic material, i.e.; rubber, the software ABAQUS was supplied with experimental uniaxial, biaxial and planar test data taken from the properties of a rubber material provided by ABAQUS manual (Habbit, Karlsson, Sorensen, Inc., 1998). Table (4.3) shows the normal stress and normal strain experimental data for the uniaxial and biaxial tests and the shear stress and shear strain experimental data for the planar test respectively. Note that no volumetric test data were given because the material is incompressible.

In order to check the stability of the material under strain, a comparison is made and its results are shown Figures (4.7, 4.8 and 4.9) for the experimental test data provided

and the ABAQUS/Standard results. This comparison showed that the material is stable for all strains and for all of the tests mentioned above (uniaxial, biaxial and planar test data). Thus, one may use these material properties for the rubber used in the rubber-steel bearing with a good confidence in the following results. Thus, for the purpose of using the proposed hyperviscoelastic model in UMAT, these material properties of rubber were conducted with some required parameter modifications.

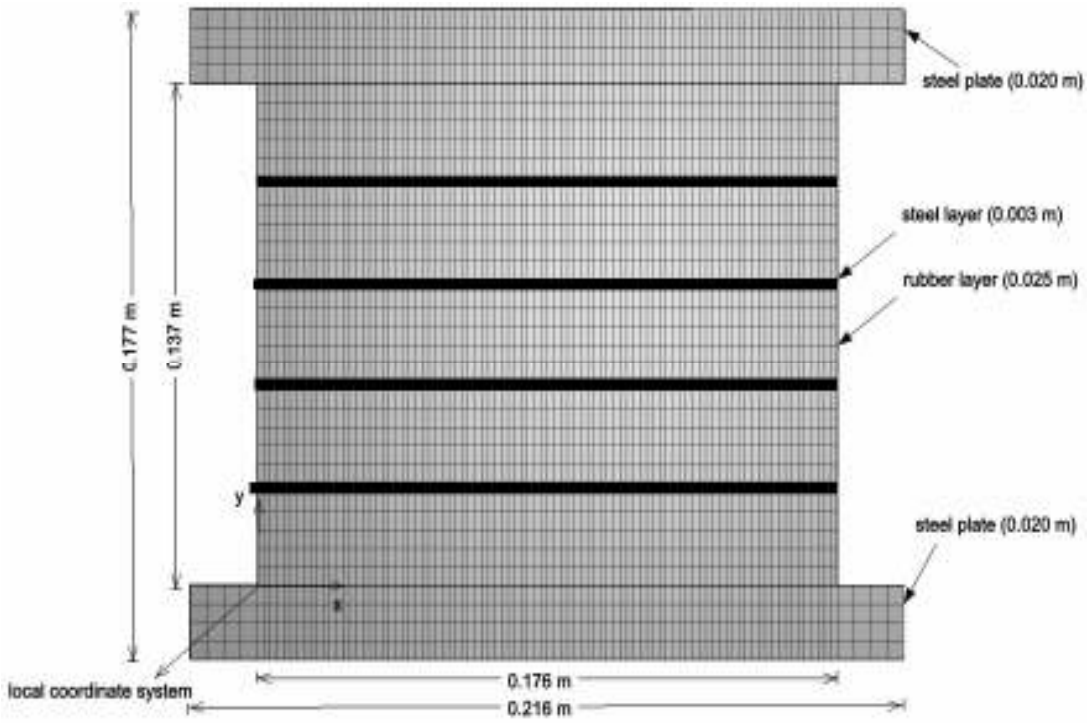

Figure 4.2: Rubber-steel bearing used for isolating the low-rise frame model.

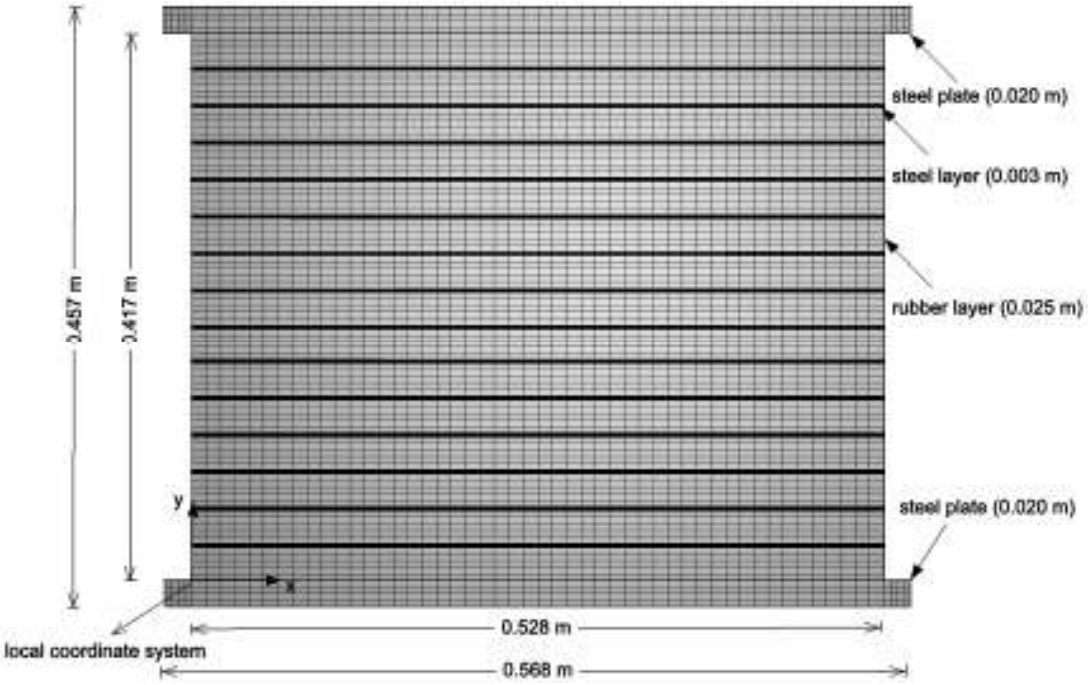

Figure 4.3: Rubber-steel bearings used for isolating the high-rise frame model.

Table 4.1 Material parameters of the rubber-steel bearings used to isolate the low-rise and high-rise frame models.

Property	Low-rise frame values	High-rise frame values
Modulus of Elasticity (E) (N/m^2)	198.252E9	198.252E9
Steel's Poisson ratio	0.2273	0.2273
Density (kg/m^3)	7800	7800

Table 4.2 Geometrical properties of the rubber-steel bearing used to isolate the low-rise and high-rise frame models.

Property	Low-rise frame values	High-rise frame values
Number of rubber layers	5	15
Number of steel layers	4	14
Thickness of each Rubber layer (m)	0.025	0.025
Thickness of each steel sheet (m)	0.003	0.003
Thickness of end steel plates (m)	0.020	0.020

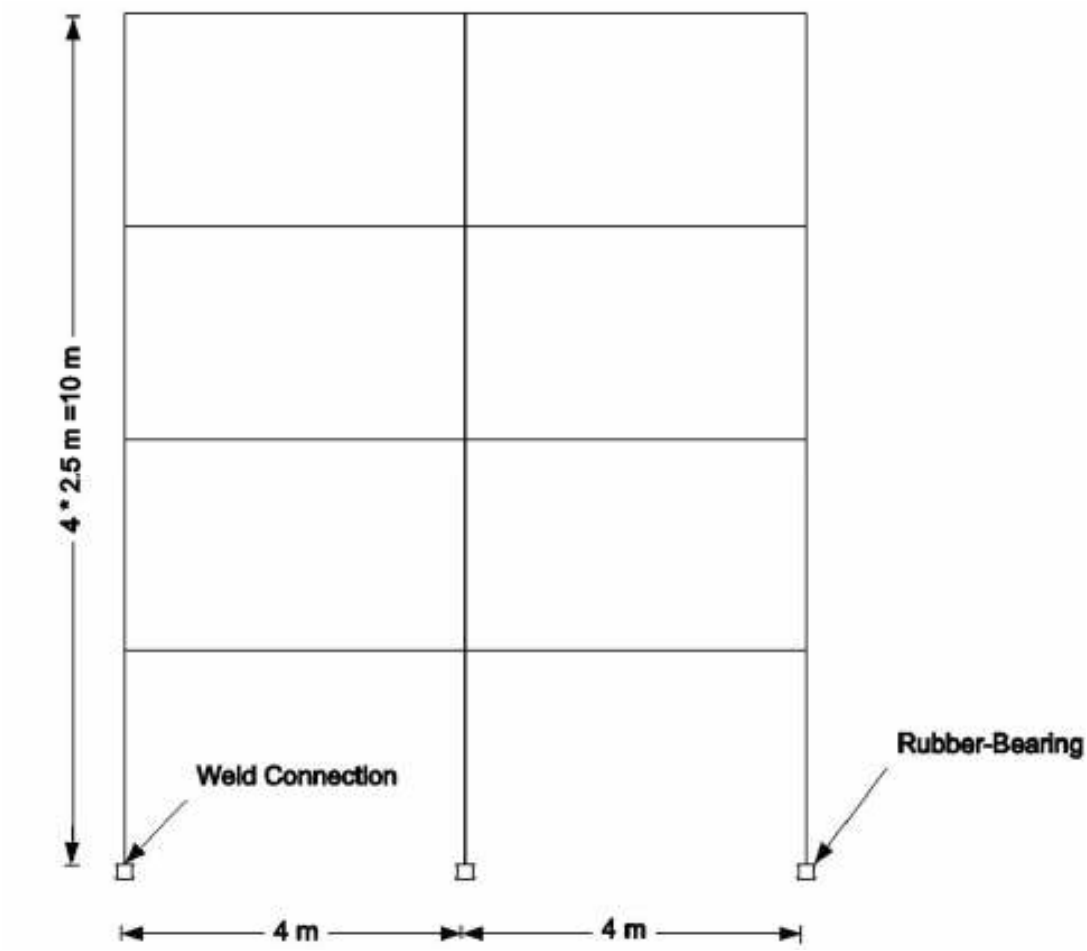

Figure 4.4: Base-isolated low-rise steel frame model.

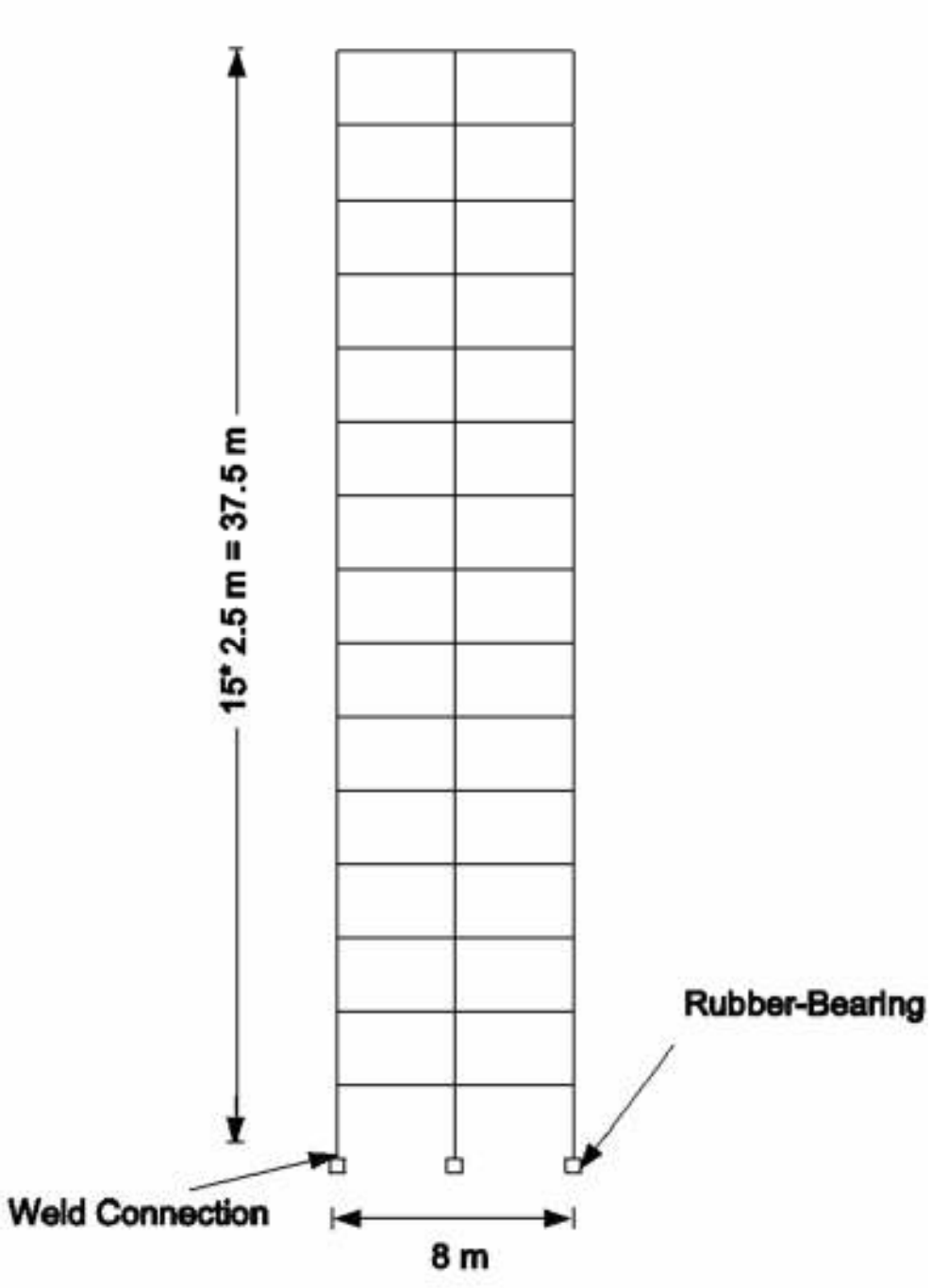

Figure 4.5: Base-isolated high-rise steel frame model.

Table 4.3 Uniaxial, Biaxial and Planar test data for the rubber material provided by ABAQUS.

Uniaxial		Biaxial		Planar (Pure shear)	
Normal Stress (MPa)	Normal strain	Normal Stress (MPa)	Normal strain	Shear Stress (MPa)	Shear strain
0.054	0.0380	0.089	0.0200	0.055	0.0690
0.152	0.1338	0.255	0.1400	0.324	0.2828
0.254	0.2210	0.503	0.4200	0.758	1.3862
0.362	0.3450	0.958	1.4900	1.269	3.0345
0.459	0.4600	1.703	2.7500	1.779	4.0621
0.583	0.6242	2.413	3.4500		
0.656	0.8510				
0.730	1.4268				

After: ABAQUS/CAE User's Manual, Version 6.4, Hibbitt,Karlsson and Sorensen, Inc., 2003.

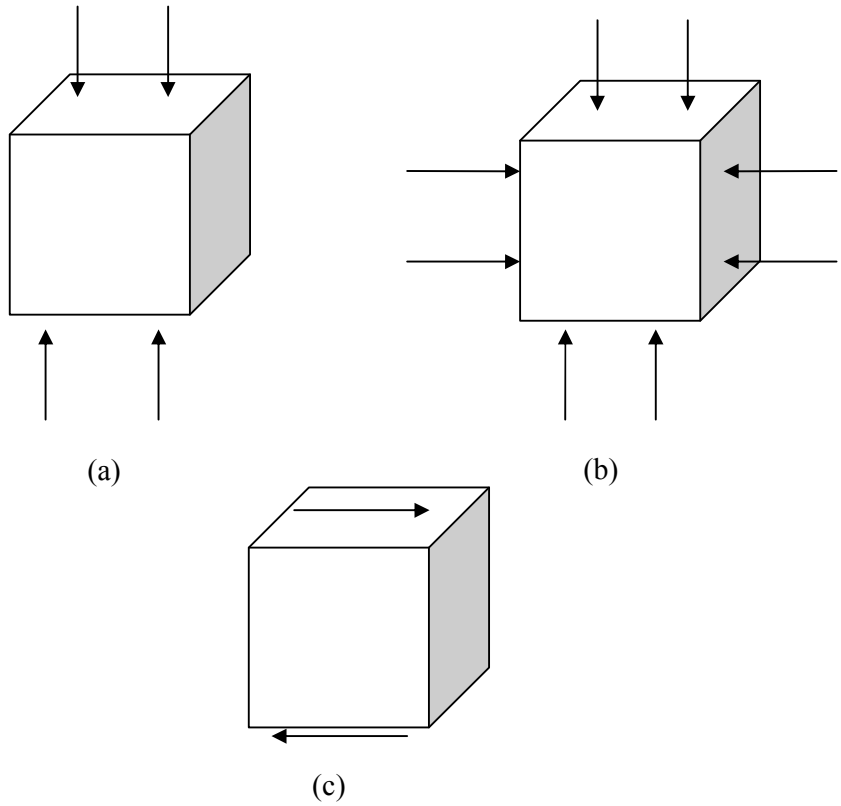

Figure 4.6: Tests performed for the rubber material provided by ABAQUS. (a) Uniaxial test (b) Biaxial test (c) Planar test.

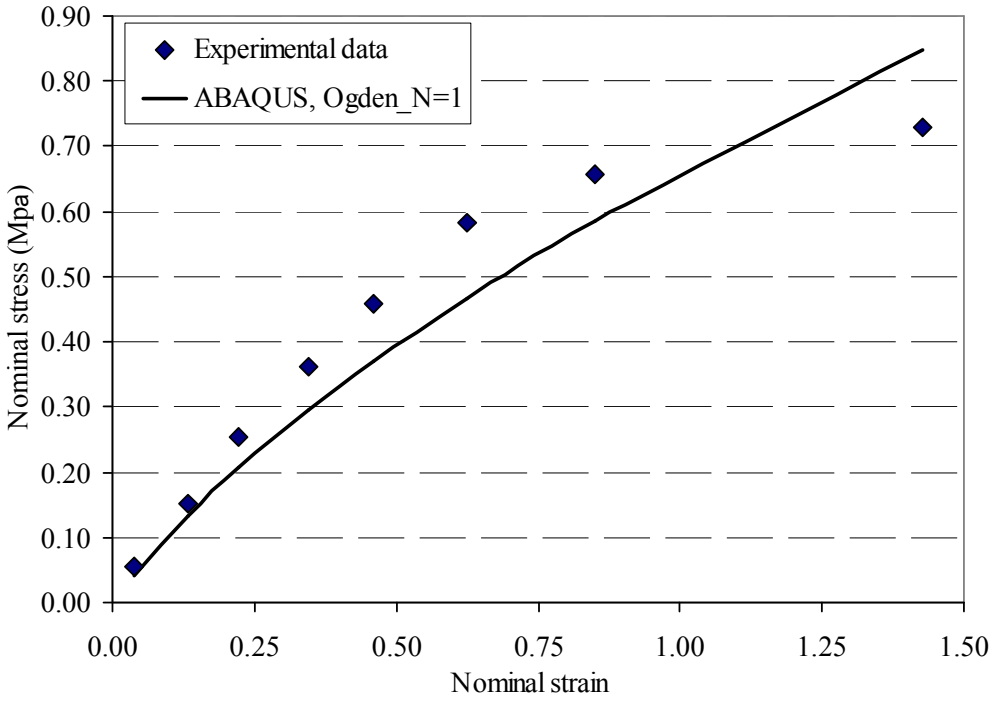

Figure 4.7: Nominal stress vs. nominal strain for a uniaxial test of rubber material.

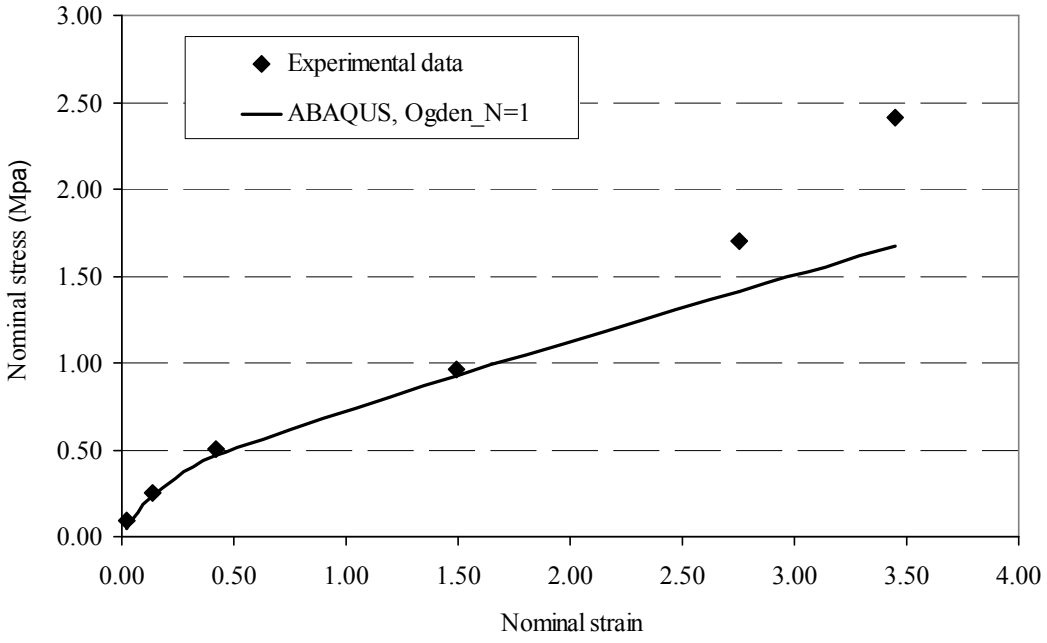

Figure 4.8: Nominal stress vs. nominal strain for a biaxial test of rubber material.

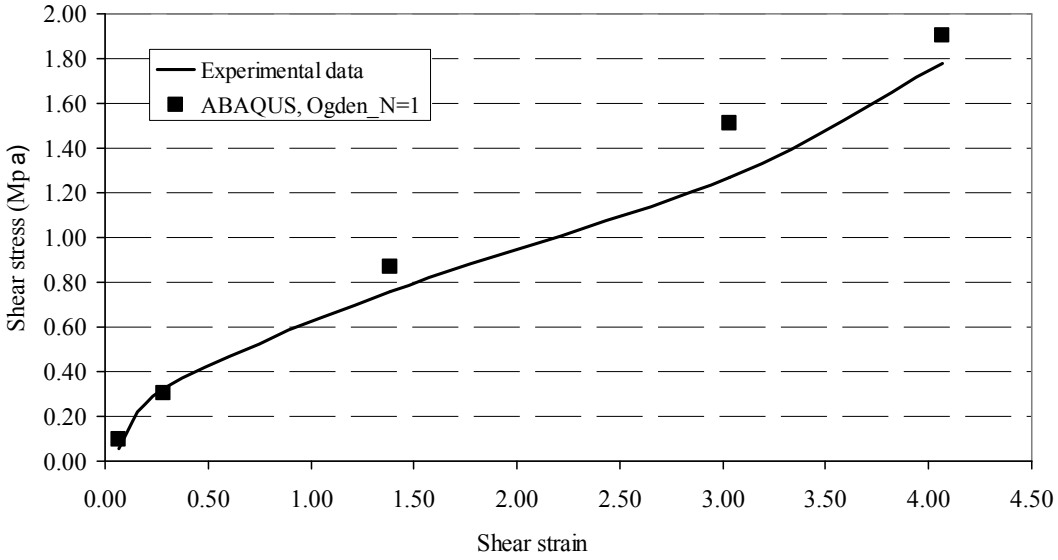

Figure 4.9: Shear stress vs. shear strain for a planar test of rubber material.

4.3 Rubber Bearing Connection

Connectors are used to model and represent either the connection between two points in an assembly or the connection between an element and the ground. The connector imposes the kinematic constraints at the point of attachment and models the mechanical properties and relationships between the attached points.

Modeling the connection between the rubber-steel bearings and the steel frame structure required using a special type of connectors that represents the required kinematic constraints. The WELD connection that is shown in Figure (4.10) is selected as the best connector found in the library of ABAQUS software. Its performance has been examined and validated against other types of connection procedures.

4.3.1 Major Connection Types in ABAQUS Library

In order to create the connector properties, two connection types can be used. These are:

1. Basic connections types:

   Basic connection types treat the translational and rotational degrees of freedom separately. They include translational types and rotational types.

   Translational types cope with the translational degrees of freedom at both ends of the connector. However, they may affect the rotational degrees of freedom at the first connector point. While rotational types, deal with the rotational degrees of freedom at both sides of the connector.

2. Assembled connection type:

   In order to have some connections that have the properties of more than one basic type, assembled connection types were introduced. They are assemblages or combinations that have previously defined properties. For example, by using a combination of the LINK, SLOT and ALIGN basic connection types, a BEAM

connection is created. The LINK connection is used in this assembled type to keep the distance between the two nodes constant by providing a pinned rigid link between them. While, in order to have the second node stay on a line that is defined by the first node and the initial position of the second node, the SLOT connection is used.

The LINK and SLOT components control the translational degrees of freedom. In order to control the rotational degrees of freedom, the ALIGN connection which provides a connection between two nodes that aligns their local directions is used.

4.3.2 WELD Connection

WELD in ABAQUS is an assembled connection type that is equivalent to combining JOIN and ALIGN basic types. While the ALIGN connection controls the rotational degrees of freedom setting them equal to zero, the JOIN connection provides the fixation of the translational degrees setting them also to zero.

The WELD connection type gives a fully bonded connection by joining the positions of two nodes (compelling kinematic constraints) and aligning their local axis directions. Moreover, it presents the actual case of practice in connection of the rubber-steel bearing system with the structural members.

4.3.3 TIE Constraint

In order to validate the results obtained when the WELD connection is used, the TIE constraint which applies the same constraints on the degrees of freedom is applied for the same models adopted previously. TIE constraint is used to avoid having a relative motion between two different surfaces that are connected (tied) together or between a point and a surface's elements. In other words, it provides a fully bonded connection between two different surfaces or between a surface and a node in such a way that the translational and rotational degrees of freedom are both tied.

In this study, the TIE constraint is used in order to tie a node to the surfaces of the two elements connected to it from both sides. This node is the one that is connecting the steel frame to the rubber-steel bearing and it is tied here to the surfaces of the two elements of the rubber-steel bearing connected to this node.

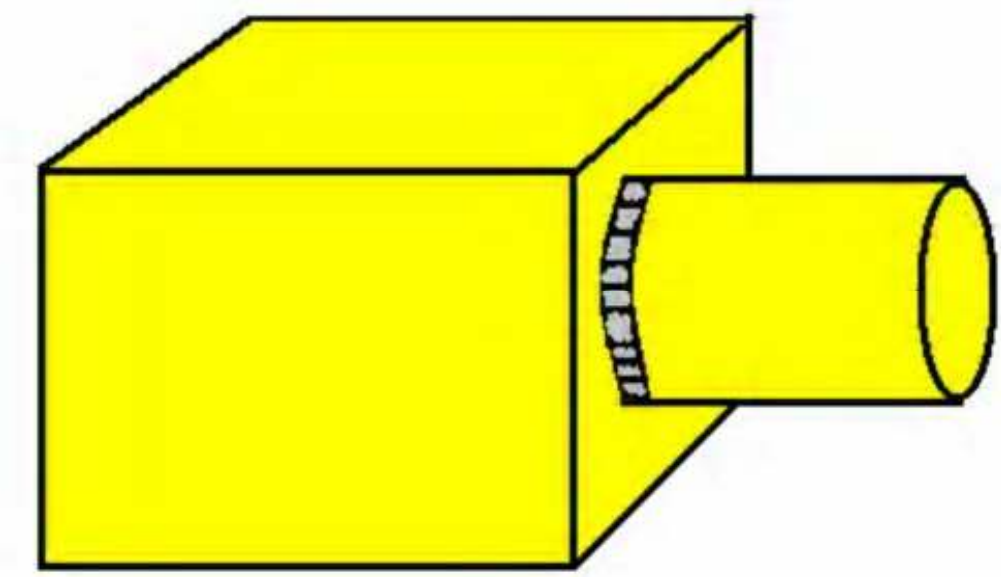

Figure 4.10: WELD connection in ABAQUS.

4.4 Description of the Fixed-Base and Base-Isolated Steel Frame Structures

4.4.1 Low-Rise Frame Model

The seismic performance of a base-isolated low-rise steel frame shown in Figure (4.4) is compared with a similar fixed-base one. Both frames are subjected to the El-Centro, N-S earthquake shown previously in Figure (1.1). In order to perform a comparison of their behavior when they are subjected to a seismic excitation, many responses have been considered. These are: the horizontal acceleration, the horizontal displacement, the relative horizontal displacement, horizontal force versus floor number, lateral force versus lateral displacement and the reaction force. These responses were chosen because of their good indication on the structural damage that might occur to the structure.

The frame is selected to have two spans (i.e.; two bays) with a four-story height. Each span is 4 m wide while the floors are 2.5 m high each. All columns have been selected to have the same geometric properties as shown in Table (4.4). This is the case also for all beams as shown in the same table. The base-isolated frame is supported on the rubber bearing shown in Figure (4.2).

Finer meshes help to obtain more accurate results. It is found that discretizing the frame members to four beam elements gives sufficient and more accurate results.

4.4.2 High-Rise Frame Model

The seismic performance of a base-isolated high-rise steel frame shown in Figure (4.5) is compared with a similar fixed-base one. Both frames are subjected to the El-Centro, N-S earthquake excitation. In order to perform a comparison of the seismic performance, many responses have been considered. These are: the horizontal acceleration, the horizontal displacement, the relative horizontal displacement, horizontal force versus

floor number, lateral force versus lateral displacement and the reaction force. These responses were chosen because of their good indication on the structural damage that might occur to the structure.

The frame is selected to have two spans with a fifteen-story height. Each span is 4 m wide while the floors are 2.5 m high each. All columns have been selected to have the same geometric properties as shown in Table (4.5). This is the case also for all beams as shown also in the same table. The base-isolated frame is supported on the rubber-steel bearing shown in Figure (4.3) with the specifications listed in Table (4.2) beside those listed in Table (4.3) for the uniaxial, biaxial and planar test data for the hyperelastic rubber material.

Finer meshes help to obtain more accurate results. It is found that discretizing the frame members to four beam elements gives sufficient and more accurate results.

Table 4.4 Geometrical properties of beams and columns of the low-rise frame model.

Property		Columns	Beams
Section type		Box	Box
Section Dimensions (*m*)	Width	0.35	0.20
	Height	0.35	0.25
	Thickness	0.04	0.025
Modulus of Elasticity, ***E***, (*Pa*)		200E9	200E9
Poisson ratio		0.25	0.25
Density (kg/m^3)		7800	7800

Table 4.5 Geometrical properties of beams and columns of the high-rise frame model.

Property		Columns	Beams
Section type		Box	Box
Section Dimensions (*m*)	Width	0.50	0.20
	Height	0.50	0.25
	Thickness	0.04	0.025
Modulus of Elasticity, ***E***, (*Pa*)		200E9	200E9
Poisson ratio		0.25	0.25
Density (kg/m^3)		7800	7800

Chapter Five

RESULTS AND DISCUSSION

5.1 Overview

The responses of the isolated and fixed-base four-story and fifteen-story structures are investigated and compared by computing several variables such as the acceleration, the displacement and the maximum inter-story displacement. For example, in order to measure the structural damage that might happen, the floors acceleration should be computed.

ABAQUS is used in the seismic analysis which is performed using the El-Centro, N-S, acceleration history, which is discretized every 0.01 second as shown previously in Figure (1.1). The time history analysis performed is an implicit dynamic one using a direct integration approach. Due to the full nonlinearity, a general dynamic fully nonlinear analysis is performed to calculate the transient dynamic response of the system. This general direct integration method is called Hilber-Hughes Taylor operator which is an extension of the trapezoidal rule with the operator parameter α is set to be -0.01. This operator is unconditionally stable and has no numerical damping.

Rubber steel bearing is the base isolation system that is used to uncouple the steel frame structure from the seismic ground motion. This is a very effective system in sustaining large displacements in shear and high loads in compression (i.e., large horizontal displacement and high vertical stiffness).

A WELD connection type is used to connect the rubber bearings to the steel frame structures. This is an assembled rigid connection that provides the required kinematic constraints. In order to confirm the results obtained when using the WELD connection,

the results are compared to these obtained by using the tie constraint which applies the same kinematical constraints as the WELD connection.

5.2 Rubber-Steel Bearing Models and Verification

In order to validate the results obtained for the hyperelastic behavior of the rubber material, a comparison is carried out between the ABAQUS/STANDARD results obtained for the rubber material and the results obtained from using a three-dimensional constitutive model of hyperviscoelasticity in large strain that is implemented as a user-defined material subroutine in ABAQUS (i.e.; UMAT) (Al-Shatnawi, 2001). The comparison covers the results obtained for the rubber-bearing model that is used for isolating the high-rise frame structure when subjected to the El-Centro earthquake. These results include stresses, displacement and acceleration.

Figures (5.1) and (5.2), show the stresses distribution (σ_{11} and σ_{22}, respectively) along the elements at the bottom of the lower steel plate when ABAQUS/STANDARD large strain model was used in expressing the rubber material. They are compared to the stresses distribution (σ_{11} and σ_{22}, respectively) along the elements at the bottom of the lower steel plate when the hyperviscoelastic material model was implemented and used as a user-defined material subroutine in ABAQUS (i.e.; UMAT). In order to validate the results obtained for the rubber material when dealing with stresses, they are both plotted at the time of maximum acceleration (i.e.; 2.02 seconds). The results obtained showed identical behavior and good agreement when using either the ABAQUS/Standard model or when using the user-defined material subroutine UMAT.

Figure (5.3) shows the acceleration in the x-direction of the upper right node of the rubber bearing model versus time which is discretized every 0.01 second. It shows

good agreement between using the Ogden model of ABAQUS and the proposed hyperviscoelastic model implemented as a UMAT.

In Figure (5.4), the horizontal displacement of the upper right node when using the ABAQUS/STANDARD for describing the rubber material is compared to the horizontal displacement at the same node when using the user-defined material subroutine UMAT. The results obtained show identical behavior when using either the ABAQUS/STANDARD or when using the user-defined material subroutine UMAT.

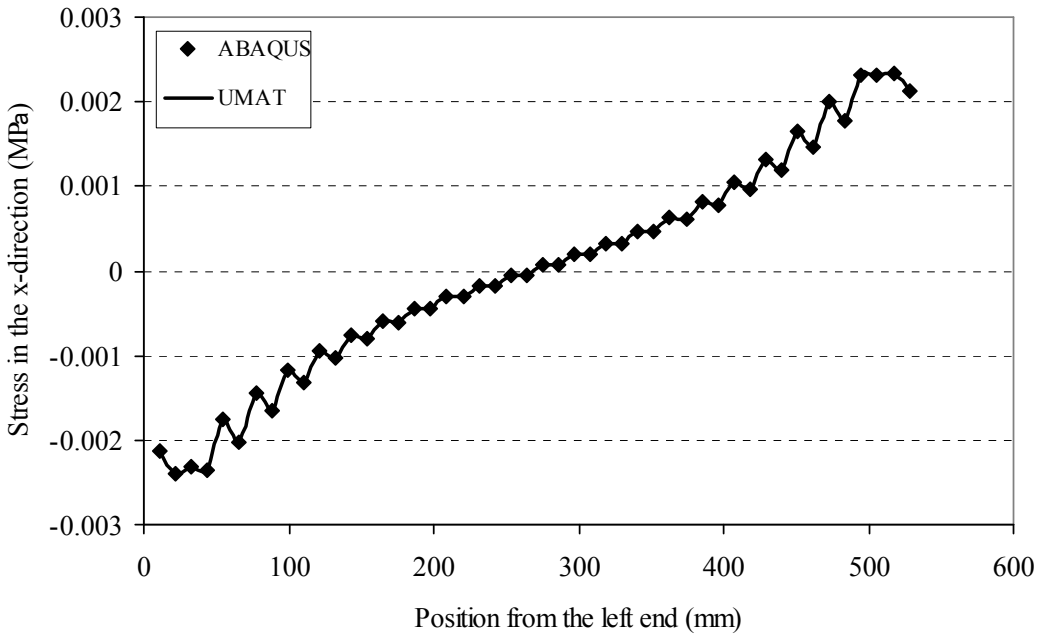

Figure 5.1: Stress in the x-direction versus the position from the left end at the bottom of the rubber-steel bearing.

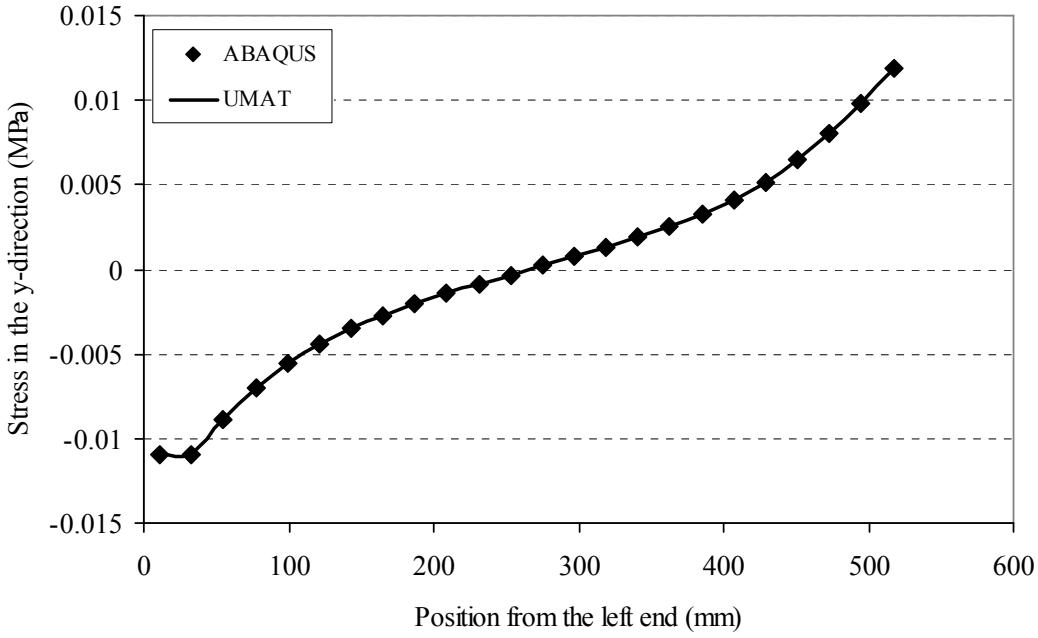

Figure 5.2: Stress in the y-direction versus the position from the left end at the bottom of the rubber-steel bearing.

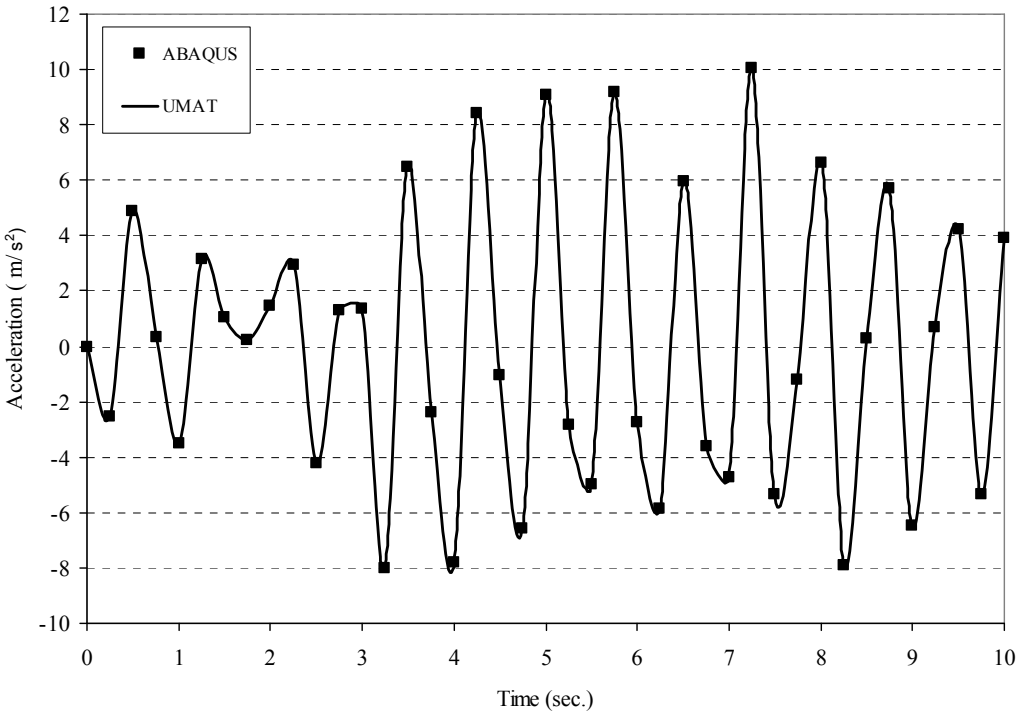

Figure 5.3: Horizontal acceleration versus time of a node located at the upper-right corner of the rubber-steel bearing.

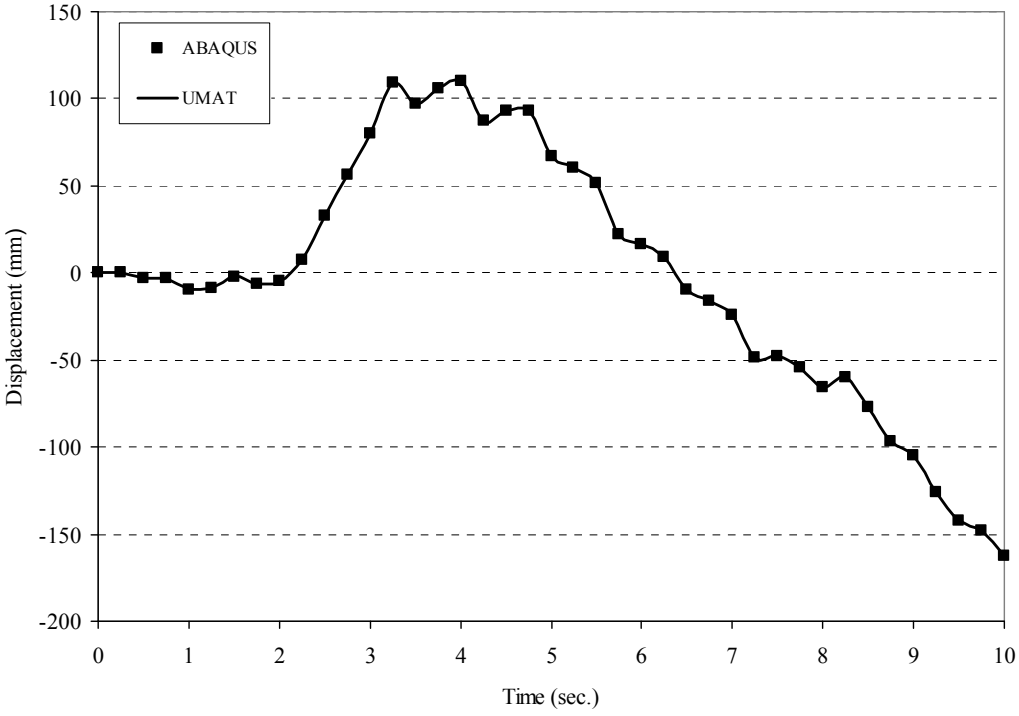

Figure 5.4: Horizontal displacement versus time of a node located at the upper-right corner of the rubber-steel bearing.

5.3 Low-Rise Frame Model

Floor acceleration affects the comfort of people and plays a significant role in increasing or decreasing the damage to the building installations; decreasing the acceleration decreases the damage of the structural members. In Figure (5.5), and in order to investigate the effect of inserting the rubber-steel bearings on the behavior of the low-rise frame model when it is subjected to the El-Centro, N-S earthquake, the horizontal acceleration of the upper right node in the low-rise isolated frame is plotted versus time that is discretized every 0.01 second. Then, it is compared to the horizontal acceleration of the same node when the frame is totally fixed without using rubber bearings. The Figure shows a high efficiency of using the rubber-steel bearing in elongating the building period and reducing the acceleration. Acceleration in the x-direction dropped significantly over the entire time. This means that the damage to the frame's structure will decrease and more efficient design is approached.

Figure (5.6) shows the horizontal displacement versus time of the upper-right node in the low-rise base-isolated frame for both WELD and TIE connections. It is compared to the horizontal displacement of the same node when the frame is totally fixed without using the rubber bearing isolation. From the figure, it is seen that the maximum horizontal displacement has not affected much over time. However, it's variation over time decreased slightly when using the rubber bearings. Consequently, the period was elongated when the frame was isolated. Thus, the structural damage was reduced.

Relative displacement is an important parameter in measuring the structural damage. As the relative displacement decreases, less structural damage occurs. In Figure (5.7), relative displacement of the upper right node in the low-rise isolated frame is plotted over time. And then, it is compared to the relative displacement of the same node when the frame is totally fixed without rubber bearings. It is clearly seen that isolating

the low-rise frame model helped in decreasing the relative horizontal displacement efficiently. Moreover, the period was elongated when the isolation system was used leading to less structural damage.

Figures (5.8) and (5.9) show the horizontal force plotted against the floor number at the right side of the frame for the low-rise fixed-base and the low-rise base-isolated frames, respectively. From both Figures, it is seen that the horizontal force at higher floors is much higher than the horizontal forces at lower floors. Moreover, the horizontal forces decreases when the high-rise frame is base isolated. This shows the good effect of using the rubber-steel bearing isolation in reducing the lateral forces act on the structure.

Lateral force is plotted against the lateral displacement in Figures (5.10 and 5.11) for a node located at the upper-right corner of the low-rise fixed-base and the low-rise base-isolated frame models respectively. From both Figures, it is clearly seen that the energy loops became much smaller when using the rubber-bearings. This happened due to the large decrease in the lateral force values.

In Figure (5.12), the reaction force in the horizontal direction at the right side base node in the low-rise base-isolated frame is compared to the reaction force in the horizontal direction of the same node when the frame is totally fixed without using rubber bearings. They are both plotted over time. It is clear that using the rubber-steel bearings gives excellent effect in reducing the reaction force. Reaction force in the y-direction dropped significantly over the entire time.

Using either the WELD connection or the tie constraint for isolating the low-rise frame model gave identical results for the horizontal acceleration, horizontal displacement, relative displacement, floor number versus the horizontal force, lateral force versus the lateral displacement and the reaction force in the x-direction versus time. This validates the results obtained for those types of connections.

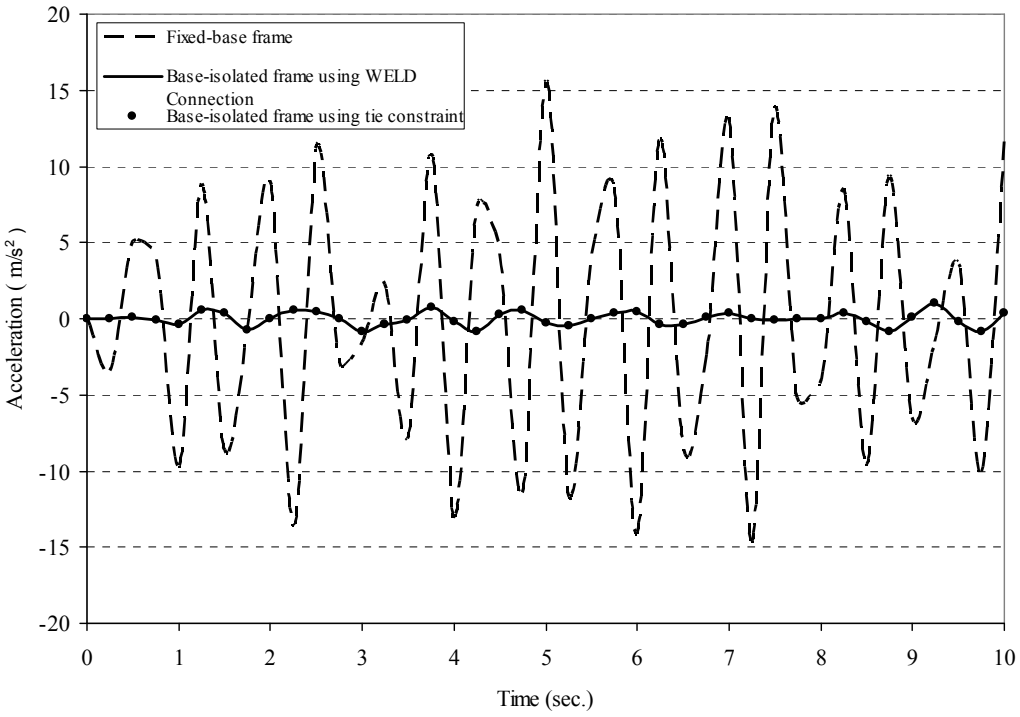

Figure 5.5: Horizontal acceleration versus time for a node located at the upper-right corner of the fixed-base and base-isolated low-rise frame models.

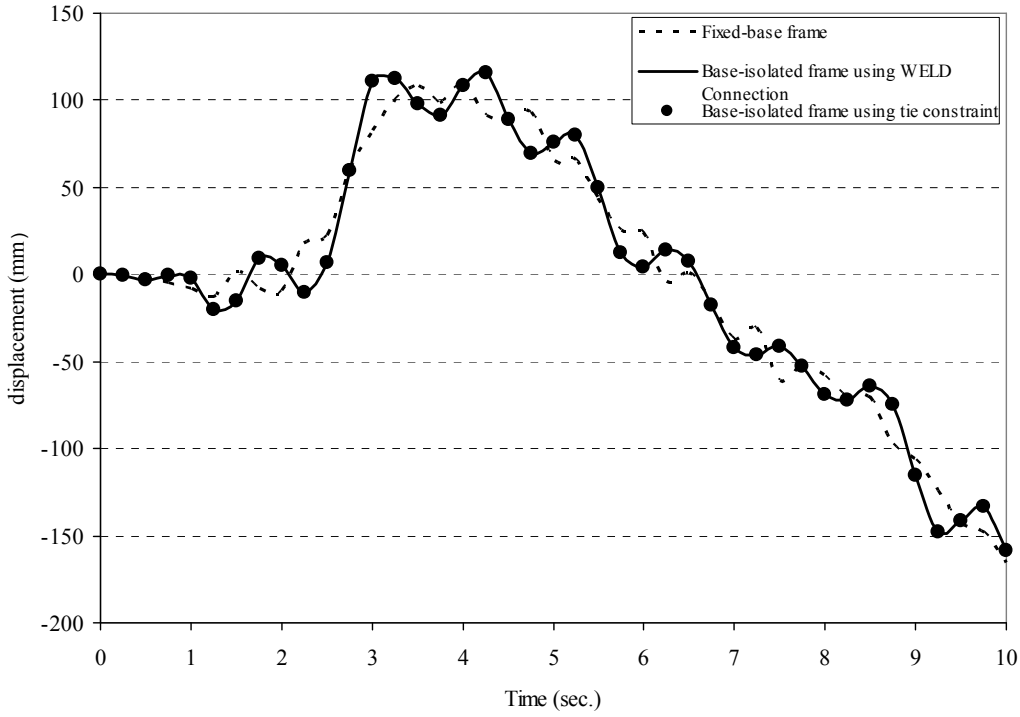

Figure 5.6: Horizontal displacement versus time for a node located at the upper-right corner of the fixed-base and base-isolated low-rise frame models.

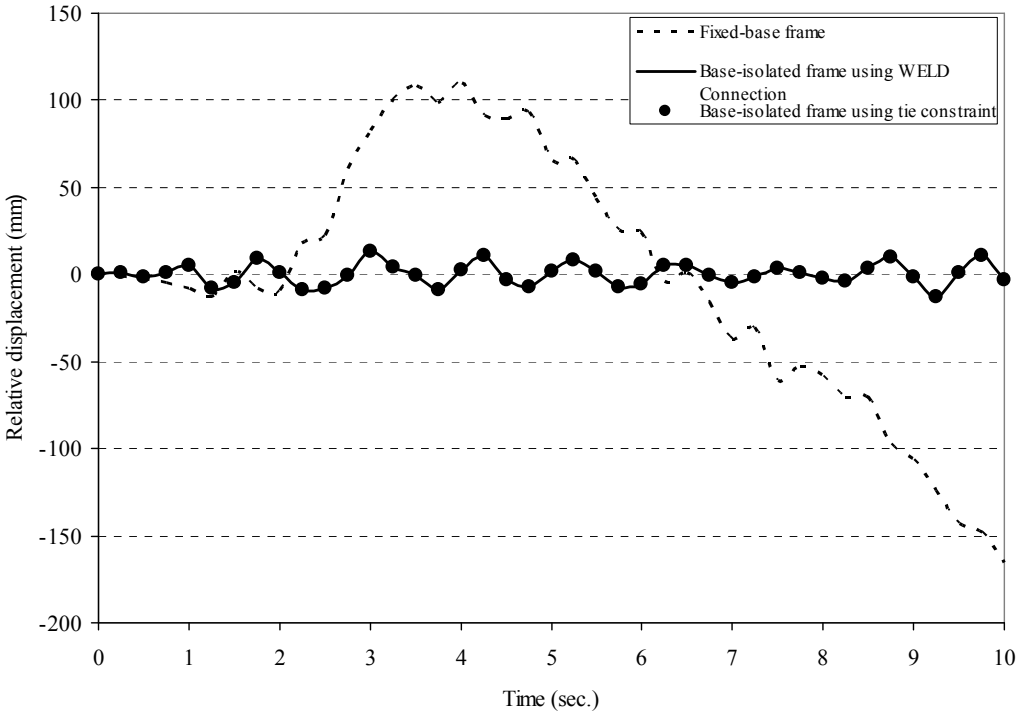

Figure 5.7: Relative displacement versus time of a node located at the upper-right corner of the fixed-base and base-isolated low-rise frame models.

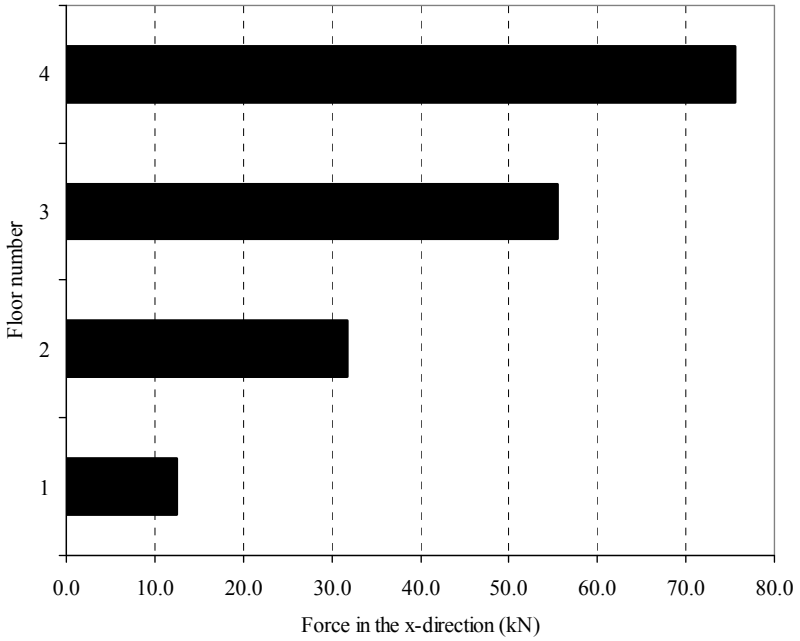

Figure 5.8: The floor number versus the horizontal force for the fixed-base low-rise frame model.

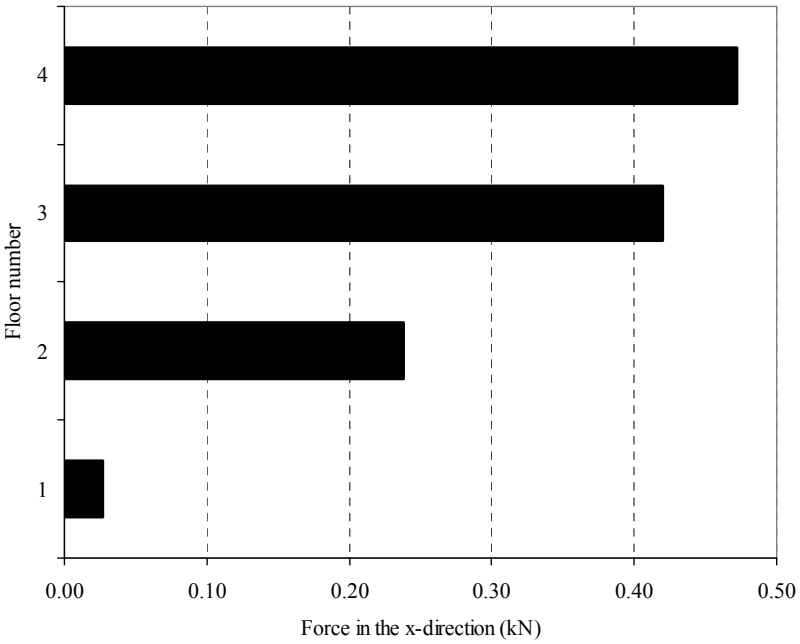

Figure 5.9: The floor number versus the horizontal force for the base-isolated low-rise frame model.

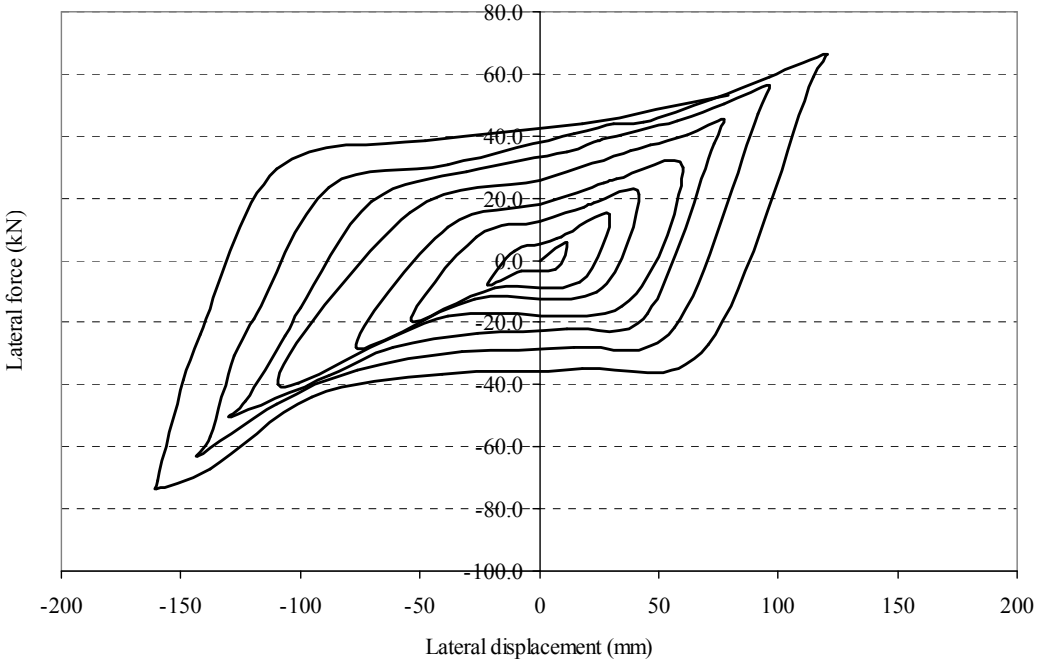

Figure 5.10: Lateral force versus the lateral displacement for a node located at the upper right corner of the fixed-base low-rise frame model.

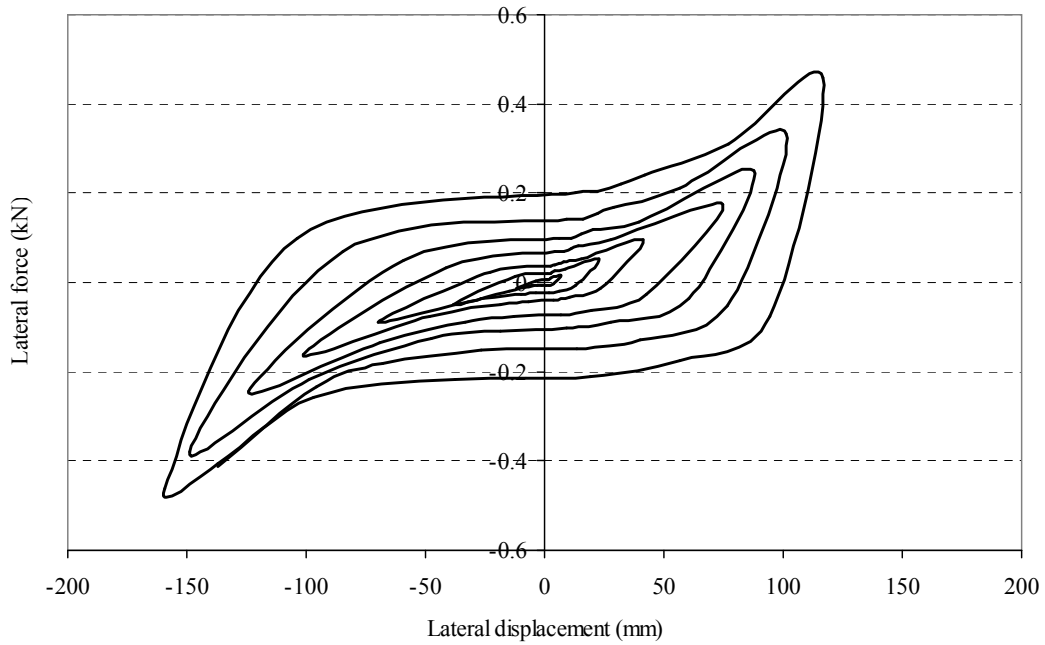

Figure 5.11: Lateral force versus the lateral displacement for a node located at the upper-right corner of the base-isolated low-rise frame model.

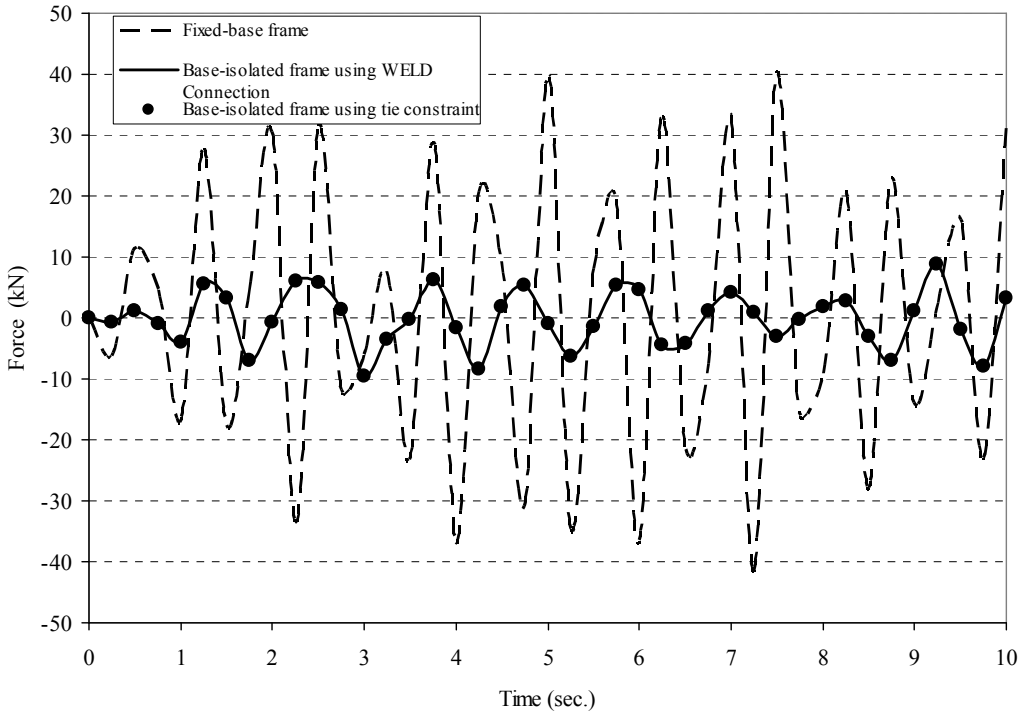

Figure 5.12: Reaction force in the x-direction versus time for a node located at the lower-right corner of the fixed-base and base-isolated low-rise frame models.

5.4 High-Rise Frame Model

In Figure (5.13), and in order to investigate the effect of inserting the rubber-steel bearings on the behavior of the high-rise frame model when it is subjected to the El-Centro, N-S earthquake, the horizontal acceleration of the upper right node in the high-rise isolated frame is plotted versus time that is discretized every 0.01 second. Then, it is compared to the horizontal acceleration of the same node when the frame is totally fixed without using rubber bearings. The Figure shows a high efficiency of using the rubber-steel bearing in elongating the building's period and reducing the acceleration. Acceleration in the x-direction dropped significantly over the entire time. This means that the damage to the frame's structure will decrease and more efficient design is approached.

Figure (5.14) shows the horizontal displacement versus time of the upper-right node in the high-rise base-isolated frame for both WELD and TIE connections. It is compared to the horizontal displacement of the same node when the frame is totally fixed without using the rubber bearing isolation. From the figure, it is seen that the maximum horizontal displacement has not affected much over time. However, it's variation over time decreased slightly when using the rubber bearing. Consequently, the period was elongated when the frame was isolated. Thus, the structural damage was reduced.

Relative displacement is an important parameter in measuring the structural damage. As the relative displacement decreases, less structural damage occurs. In Figure (5.15), relative displacement of the upper right node in the high-rise isolated frame is plotted over time. Then, it is compared to the relative displacement of the same node when the frame is totally fixed without using rubber bearings. It is clearly seen that isolating the high-rise frame model helped in decreasing the relative horizontal

displacement efficiently. Moreover, the period was elongated when the isolation system was used leading to less structural damage.

Figures (5.16) and (5.17) show the horizontal force plotted against the floor number at the right side of the frame for the high-rise fixed-base and the high-rise base-isolated frames, respectively. From both Figures, it is seen that the horizontal force at higher floors is much larger than the horizontal forces at lower floors. Moreover, the horizontal forces decreases when the high-rise frame is base isolated. This shows the advantage of using the rubber-steel bearing isolation system in reducing the lateral forces that act on the structure.

Lateral force is plotted against the lateral displacement in Figures (5.18 and 5.19) for a node located at the upper-right corner of the high-rise fixed-base and the high-rise base-isolated frame models respectively. From both Figures, it is clearly seen that the energy loops became much smaller when using the rubber-bearings. This happened due to the large decrease in the lateral force values.

In Figure (5.20) the reaction force in the x-direction at the right side base-node in the high-rise base-isolated frame is compared to the reaction force in the x-direction of the same node when the frame is totally fixed without using the rubber bearings. They are both plotted over time. It is clear that using the rubber-steel bearings gives excellent effect in reducing the reaction force. Reaction force in the y-direction dropped significantly over the entire time.

Using either the WELD connection or the tie constraint for isolating the high-rise frame model gave identical results for the horizontal acceleration, horizontal displacement, relative displacement, floor number versus the horizontal force, lateral force versus the lateral displacement and the reaction force in the x-direction versus time. This validates the results obtained for those types of connections.

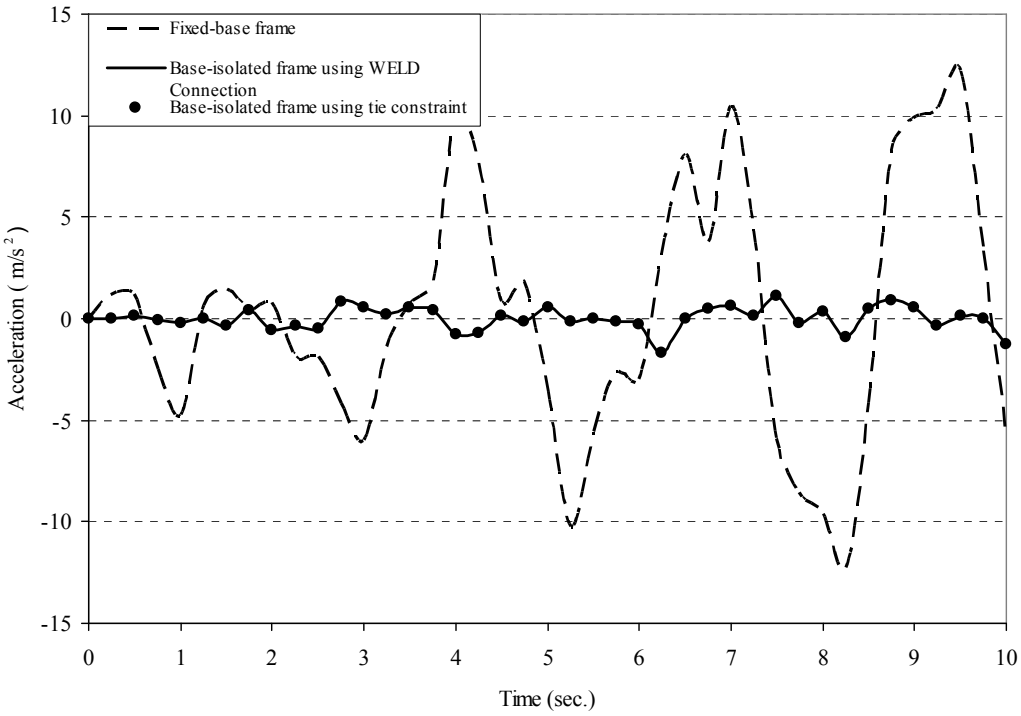

Figure 5.13: Horizontal acceleration versus time for a node located at the upper-right corner of the fixed-base and base-isolated high-rise frame models.

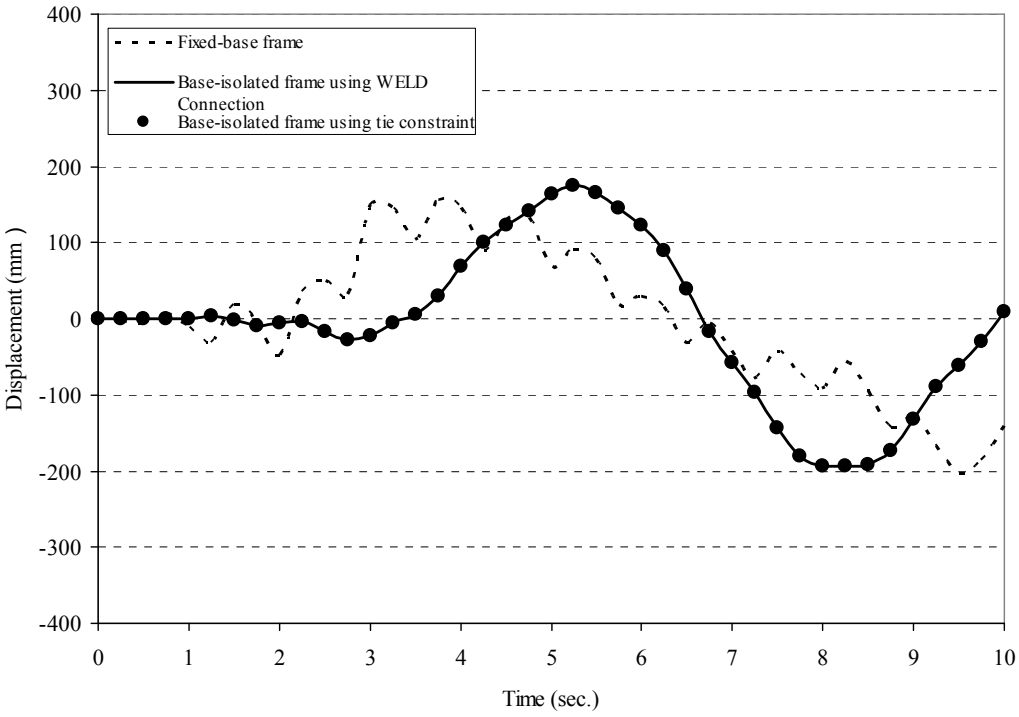

Figure 5.14: Horizontal displacement versus time for a node located at the upper-right corner of the fixed-base and base-isolated high-rise frame models.

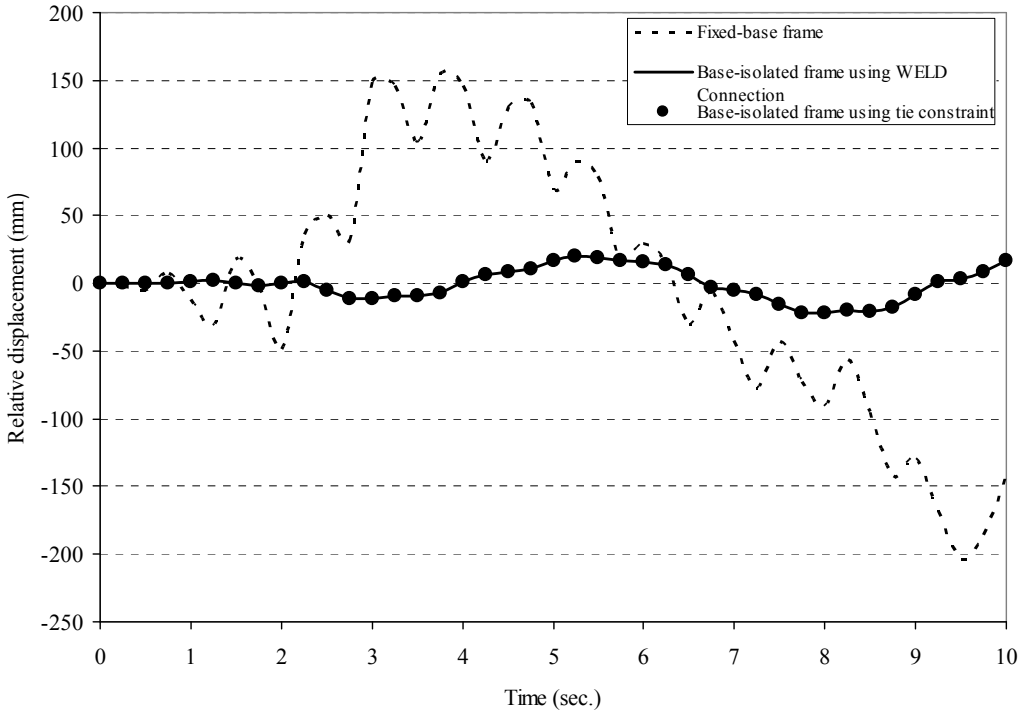

Figure 5.15: Relative displacement versus time of a node located at the upper-right corner of the fixed-base and base-isolated high-rise frame models.

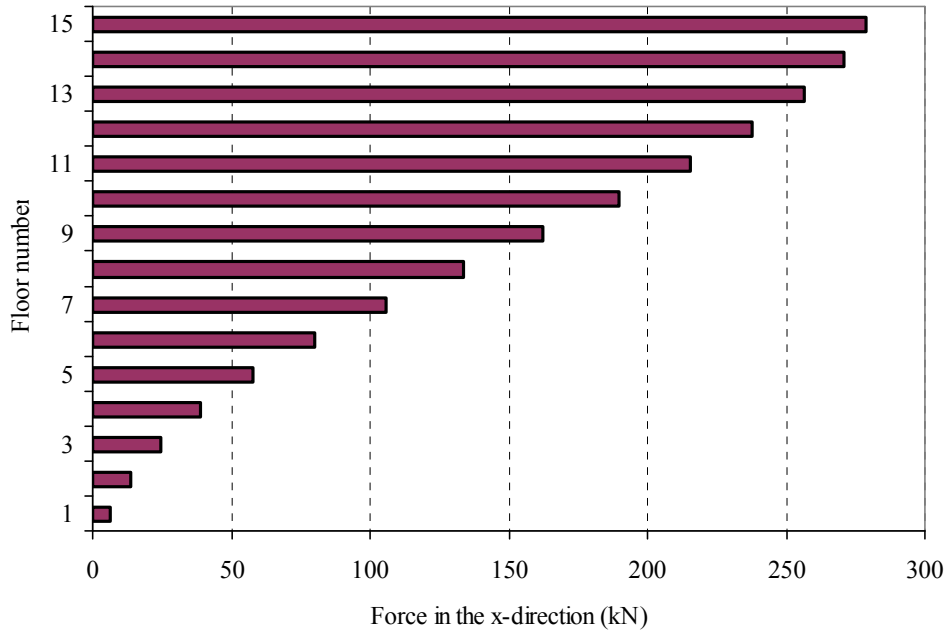

Figure 5.16: The floor number versus the horizontal force for the fixed-base high-rise frame model.

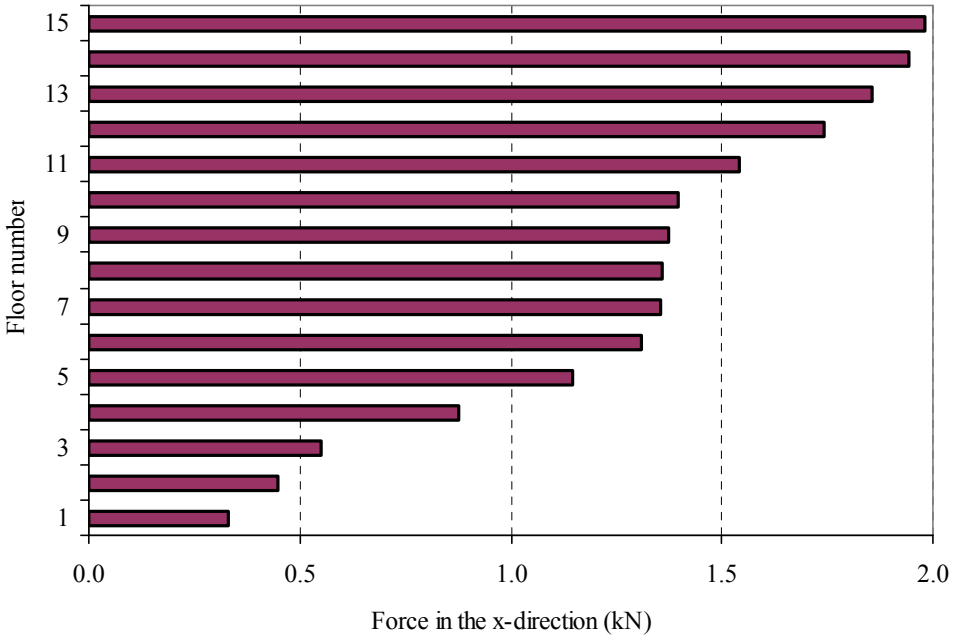

Figure 5.17: The floor number versus the horizontal force for the base-isolated high-rise frame model.

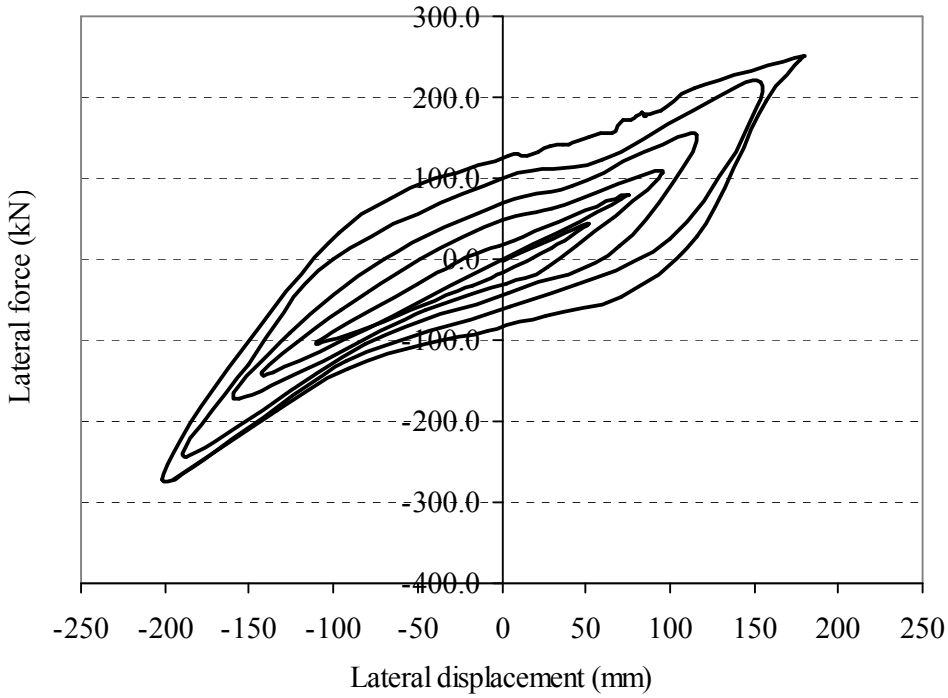

Figure 5.18: Lateral force versus the lateral displacement for a node located at the upper right corner of the fixed-base high-rise frame model.

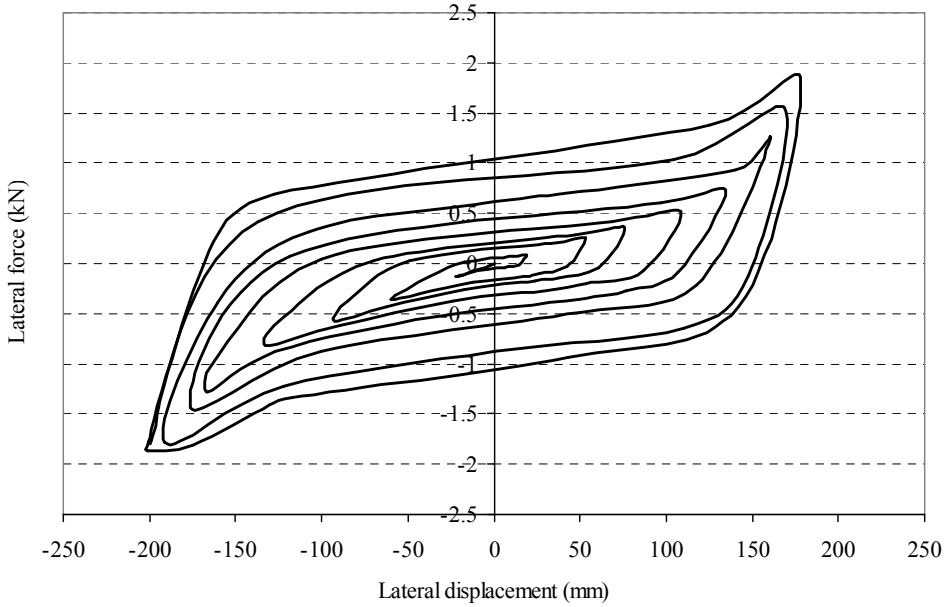

Figure 5.19: Lateral force versus the lateral displacement for a node located at the upper-right corner of the base-isolated high-rise frame model.

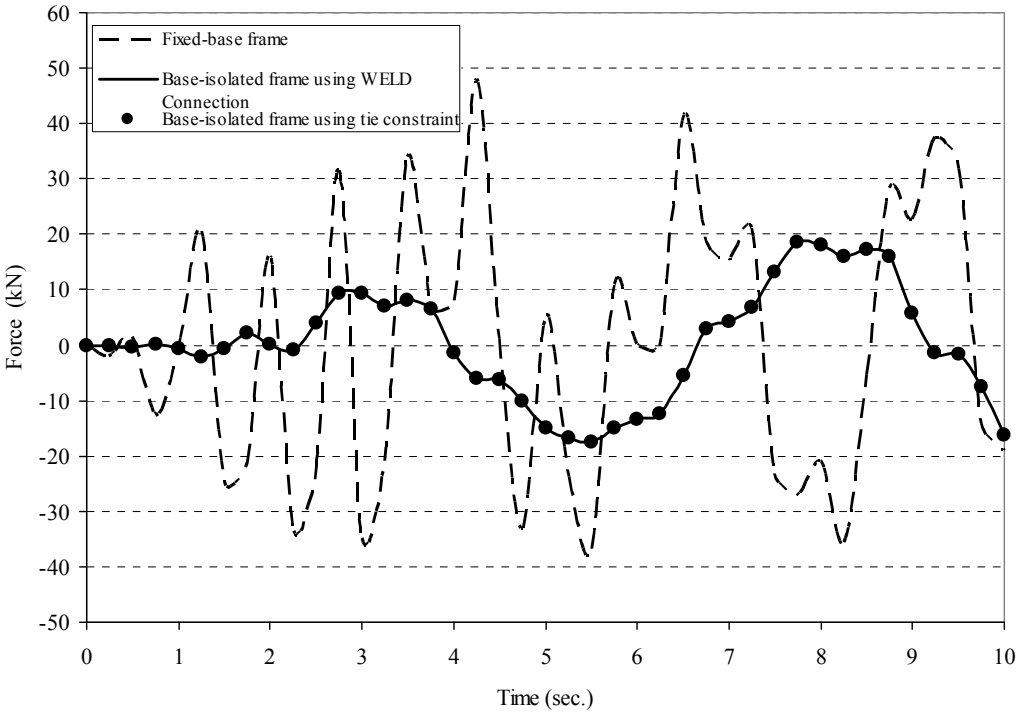

Figure 5.20: Reaction force in the x-direction versus time for a node located at the lower-right corner of the fixed-base and base-isolated high-rise frame models.

Using rubber-steel bearings as a base-isolation system to protect the low-rise and high-rise frame models from the earthquake excitation gave excellent results as discussed previously. However, the behavior of both structures was similar regarding some factors but different regarding others.

Acceleration for example, decreased significantly for both structures when they were isolated. However, although the horizontal displacement did not change much when both frames were isolated, the period of the high-rise frame increased relatively more than period of the low-rise frame. The rest of the results for the relative displacement, floor number versus the horizontal force, lateral force versus the lateral displacement and the reaction force in the x-direction versus time showed similar behavior for both structures.

This comparison shows that using rubber-steel bearings for low-rise and high-rise structures helps both of them to sustain the earthquake excitation. However, better results could be observed for the high-rise structures because their period increased relatively more than the period of the low-rise structures which reduces the effect of the earthquake excitation on this type of structures.

Chapter Six

CONCLUSIONS AND RECOMMENDATIONS

6.1 Conclusions

In the present study, the non-linear seismic responses of a fixed-base and base-isolated steel frame structures have been investigated. These structures are represented by selected models of low- and high-rise frames. Moreover, the response of the rubber-steel bearing isolation system has been studied separately and the material models of the rubber are investigated and verified. The solution for the responses of both fixed-base and base-isolated frames considering the highly non-linear characteristics of the base isolation system (rubber-steel bearings) was carried out.

The stresses, accelerations and displacements of the rubber bearing system were computed using two material models. These are a modified large strain, three-dimensional hyperviscoelastic (i.e.; time-dependent) material model (Al-Shatnawi, 2001) that is linked with ABAQUS as a user defined material model (UMAT), and another large strain hyperelastic material model exists within the software ABAQUS (i.e.; Ogden type). Based on modified material model, when the structure is subjected to El-Centro, N-S earthquake, the stresses, accelerations history and the lateral displacements of the rubber bearings are all found to have good agreement with those obtained when using the hyperelastic Ogden model of ABAQUS.

Moreover, similar responses of the fixed-base and base-isolated steel frames regarding the relative floor displacements, accelerations and some other factors are obtained and found to be in good agreement using either the WELD connection or the TIE constraint to represent the kinematic constraints at the connection point between the rubber-bearings and the frames.

Rubber-bearings showed a great efficiency in uncoupling both structures from the seismic ground motion helping both of them to sustain the earthquake excitation. This is observed by elongating the period of the structure and reducing the horizontal accelerations, lateral-forces and the relative horizontal roof displacement. However, better results are observed for the high-rise structures because their period increased relatively more than the period of the low-rise structures which reduces the effect of the earthquake excitation on this type of structures leading to less damage of the structures.

6.2 Recommendations

Many issues could be added to this work in the future to accomplish further goals. This may include the followings:

- The need for more experimental work to identify accurate non-linear parameters of the rubber bearings in order to develop more efficient mathematical constitutive models to analyze and design the isolation systems.
- Further studies are required on the failure mechanisms and collapsing of the isolation systems.
- The dynamic responses of the non-smooth friction isolators under the external excitations need to be investigated.
- More studies are required on other types of structures, e.g., reinforced concrete structures, water tanks, bridges, and others.
- Extend the research to include earthquakes effects in the vertical direction.

References

ABAQUS Analysis User's Manual, Ver. 6.4, Hibbitt, Karlsson and Sorensen, Inc., 2003.

ABAQUS Benchmarks Manual, Version 6.4, Hibbitt, Karlsson and Sorensen, Inc., 2003.

ABAQUS/CAE User's Manual, Version 6.4, Hibbitt, Karlsson and Sorensen, Inc., 2003.

ABAQUS Example Problems Manual, Version 6.4, Hibbitt,Karlsson and Sorensen, Inc., 2003.

ABAQUS Keywords Reference Manual, Version 6.4, Hibbitt,Karlsson and Sorensen, Inc., 2003.

ABAQUS Theory Manual, Version 6.4, Hibbitt,Karlsson and Sorensen, Inc., 2003.

Al-Shatnawi A.,(2001), **Developments for complex inelastic large-scale simulations and parameter estimation, with emphasis on large strain, softening and localization phenomena**, PhD Dissertation, University of Akron.

Carneiro J O, de Melo F J Q, Jalali S and Camanho P P, (2004). Analytical dynamic analysis of earthquake base–isolation structures using time history modal superposition. **Multi-body Dynamics.** vol. 218, pp 39-49.

Ceccoli C,Mazzotti C and Savoia M., (1999). Non-linear seismic analysis of base-isolated RC frame structures. **Earthquake Engineering and Structural Dynamics**, vol. 28, pp 633-653.

Chopra A. K., (1995). **Dynamic of structures**, Linköping Institute of Technology, Sweden.

Clough R. and Penzien J., (1993). **Dynamic of structures**, McGraw-Hill,Inc,Singapore.

Gendy, A.S. and Saleeb, A.F., (2000), Nonlinear material parameter estimation for characterizing hyperelatic large strain models. **Computational Mechanics**, vol.25, pp 66-77.

Hamidi M., Naggar M. H.and Vafai A., (2003). Response of structures supported on SCF isolation systems. **Earthquake Engineering and Structural Dynamics,** vol.32, pp 1555-1584.

Hart G. and Wong K., (2000). **Structural dynamics for structural engineers**, John Wiley & Sons, Inc., New York.

Hwang JS., Wu JD, Pan T-C., and Yang G., (2002). A mathematical hysteretic model for elastomeric isolation bearings. **Earthquake Engineering and Structural Dynamics**, vol. 31, pp 771-789.

Jankowski R.,(2005). Non-linear viscoelastic modelling of earthquake-induced structural pounding**. Earthquake Engineering and Structural Dynamics,** vol.34, pp 595-611.

Kikuchi M. and Aiken I., (1997). An analytical hysteresis model for elastomeric seismic isolation bearings. **Earthquake Engineering and Structural Dynamics,** vol.26, pp 215-231.

Lemaitre J. and Chaboche, (1990). **Mechanics of Solid Materials**, Cambridge University, Press, New York.

Malhotra P., (2004). Dynamics of seismic impacts in base-isolated buildings. **Earthquake Engineering and Structural Dynamics**, vol. 26, pp 797-813.

Mooney M., (1940). A theory of large elastic deformations. **J. of applied Mechanics**, vol.11, pp582-592.

Ogden, R.W., (1984). **Nonlinear elastic deformations**, Ellis Harwood, Chichester,UK.

Ordonez D, Foti D and Bozzo L., (2003). Comparative study of the inelastic response of base isolated buildings. **Earthquake Engineering and Structural Dynamics**, vol. 31, pp 771-789.

Rivlin, R.S., (1951). Large elastic deformations of isotropic materials; Part III: Experiments on the deformation of rubber. **Philos. Trans. Roy. Soc. London, Ser.A**, vol. 243, pp. 251-288.

Saleeb, A.F., Chang, T.Y.P. and Arnold, S.M., (1992). On the development of explicit robust schemes for implementations of a class of hyperelastic models in large-strain analysis of rubbers. **Int. J. Numerical Methods in Engineering**, vol.33, pp 1237-1249.

Salomon O, Oller S and Barbat A., (1999). Finite element analysis of base isolated buildings subjected to earthquake loads. **International Journal for Numerical Methods in Engineering** vol.46, pp 1741-1761.

Shrimali M.K.and Jangid R.S., (2002). Non-linear seismic response of base-isolated liquid storage tanks to bi-directional excitation. **Nuclear Engineering and Design**, vol. 217, pp 1-20.

Skinner R., Robinson W. and McVerry G., (1993). **An introduction to seismic isolation**. John Wiley & Sons, Chichester.

Tsai T. S., (1997). Finite element formulations for friction pendulum seismic isolation bearings. **International Journal for Numerical Methods in Engineering**, vol.40, pp 29-49.

UBC, **Uniform Building Code**, (1997). International Conference of Building Officials, Whittier, California.

Valanis, K.C., and Landel, R.F., (1967). The strain energy function of a hyper-elastic material in terms of extension ratios. **J. Applied Phys**., vol. 38, pp. 2997-3002.

Appendix A

SAMPLE OF ABAQUS INPUT FILES

```
*Heading
** Job name: TEST4 Model name: Model-1
*Preprint, echo=NO, model=NO, history=NO, contact=NO
** Part
*Part, name="STEEL FRAME"
*Node
      1,          4.,         10.
      2,          4.,         7.5
      3,          0.,         7.5
      4,          0.,         10.
      .           .           .
      .           .           .
      .           .           .
     23,          2.,         7.5
     24,         2.5,         7.5
     25,          3.,         7.5
      .           .           .
      .           .           .
      .           .           .

     44,          0.,         7.
     45,         4.5,         10.
     46,          5.,         10.
      .           .           .
      .           .           .
      .           .           .
     77,         5.5,         5.
     78,          6.,         5.
     79,         6.5,         5.
     80,          7.,         5.
      .           .           .
      .           .           .
      .           .           .

    105,         4.5,         2.5
    106,          5.,         2.5
    107,         5.5,         2.5
      .           .           .
      .           .           .
      .           .           .

    117,          4.,         1.5
    118,          4.,         1.
    119,          4.,         0.5
```

```
*Element, type=B21
1,  1, 16
2, 16, 17
3, 17, 18
.   .   .
.   .   .
.   .   .
22,  2, 34
23, 34, 35
24, 35, 36
25, 36, 37
.   .   .
.   .   .
.   .   .

104, 102, 103
105, 103, 104
106, 104,  13
.   .   .
.   .   .


.   .   .
123, 118, 119
124, 119,  15

*Nset, nset=BEAMS
  1,  2,  3,  4,  5,  6,  7,  8,  9, 10, 11, 12, 20, 21, 22, 23
 24, 25, 26, 27, 28, 29, 30, 31, 32, 33, 34, 35, 36, 37, 38, 39
 40, 45, 46, 47, 48, 49, 50, 51, 64, 65, 66, 67, 68, 69, 70, 75
 76, 77, 78, 79, 80, 81, 94, 95, 96, 97, 98, 99, 100, 105, 106, 107
108, 109, 110, 111
*Elset, elset=BEAMS
  6,  7,  8,  9, 10, 11, 12, 13, 14, 15, 16, 17, 18, 19, 20, 21
 22, 23, 24, 25, 26, 27, 28, 29, 35, 36, 37, 38, 39, 40, 41, 42
 58, 59, 60, 61, 62, 63, 64, 65, 71, 72, 73, 74, 75, 76, 77, 78
 94, 95, 96, 97, 98, 99, 100, 101, 107, 108, 109, 110, 111, 112, 113, 114
*Nset, nset=COLUMNS
  1,  2,  3,  4,  5,  6,  7,  8,  9, 10, 11, 12, 13, 14, 15, 16
 17, 18, 19, 41, 42, 43, 44, 52, 53, 54, 55, 56, 57, 58, 59, 60
 61, 62, 63, 71, 72, 73, 74, 82, 83, 84, 85, 86, 87, 88, 89, 90
 91, 92, 93, 101, 102, 103, 104, 112, 113, 114, 115, 116, 117, 118, 119
*Elset, elset=COLUMNS
  1,  2,  3,  4,  5, 30, 31, 32, 33, 34, 43, 44, 45, 46, 47, 48
 49, 50, 51, 52, 53, 54, 55, 56, 57, 66, 67, 68, 69, 70, 79, 80
 81, 82, 83, 84, 85, 86, 87, 88, 89, 90, 91, 92, 93, 102, 103, 104
105, 106, 115, 116, 117, 118, 119, 120, 121, 122, 123, 124
*Nset, nset=_PickedSet4, internal, generate
  1, 119,   1
*Elset, elset=_PickedSet4, internal, generate
  1, 124,   1
```

```
** Region: (ColumnSteelSec:COLUMNS), (Beam Orientation:Picked)
** Section: ColumnSteelSec  Profile: ColumnBoxProfile
*Beam Section, elset=COLUMNS, section=BOX,MATERIAL=steelF
0.35, 0.35, 0.04, 0.04, 0.04, 0.04
0.,0.,-1.
** Region: (BeamSteelSec:BEAMS), (Beam Orientation:Picked)
** Section: BeamSteelSec  Profile: BeamBoxProfile
*Beam Section, elset=BEAMS, section=BOX,MATERIAL=steelF
0.2, 0.25, 0.025, 0.025, 0.025, 0.025
0.,0.,-1.
*End Part
**
**
** ASSEMBLY
**
*Assembly, name=Assembly
**
*Instance, name="STEEL FRAME-1", part="STEEL FRAME"
*End Instance
**
*Nset, nset=FIXED, instance="STEEL FRAME-1"
 13,14,15
*Nset, nset=LEFT, instance="STEEL FRAME-1"
5,7,9,11,13
*Nset, nset=MIX, instance="STEEL FRAME-1"
5,7,9,11,13,14,15
*Nset, nset=SIDE, instance="STEEL FRAME-1"
 7,13
*elset, elset=ALL, instance="STEEL FRAME-1", generate
 1,  124,  1
**
*End Assembly
*Amplitude, time=TOTAL TIME, value=RELATIVE, input=QUAKE.AMP, NAME=EQ
**
** MATERIALS
**
*Material, name=steelF
*Density
7800.,
*Elastic
 2e+11, 0.25
**
** BOUNDARY CONDITIONS
**
** Name: FIXED Type: Displacement/Rotation
*Boundary
FIXED, 2, 2
FIXED, 6, 6
** ----------------------------------------------------------------
**
```

```
** STEP: DYNAMIC STEP
**
*Step, name="DYNAMIC STEP", nlgeom=NO, inc=1000
EARTHQUAKE ACCELERATION
*Dynamic,alpha=-0.05,direct
0.01,10.0,
**
** BOUNDARY CONDITIONS
**
** Name: DYNAMIC Type: Acceleration/Angular acceleration
*Boundary, amplitude=EQ, type=ACCELERATION
FIXED, 1, 1, 9.81
**
** OUTPUT REQUESTS
**
*Restart, write, frequency=25
*PRINT,RESIDUAL=NO,FREQUENCY=10
*NODEPRINT,FREQUENCY=10, nset=FIXED
RF
*ENERGY FILE,FREQUENCY=1
*OUTPUT,FIELD,FREQUENCY=1,OP=NEW
*NODE OUTPUT,nset=FIXED
RF
*ELEMENT OUTPUT,elset=ALL, POSITION=NODES
SF,S
*OUTPUT,HISTORY,FREQUENCY=25,OP=NEW
*NODE OUTPUT, nset=FIXED
RF
*NODE OUTPUT, nset=SIDE
U,A
*ELEMENT OUTPUT,elset=ALL
SF,S
*ENERGY OUTPUT,VARIABLE=ALL
*END STEP
```

الاستجابة الزلزالية اللاخطية للمباني الهيكلية المعزولة القواعد باستخدام الدعامات المطاطية

إعداد
اياد منذر سلامة العمارين

المشرف
ا.د. عبد القادر النجمي

المشرف المشارك
د. انيس شطناوي

ملخص

حصل الكثير من التقدم في البحث و التطبيق لعزل قواعد الأبنية لجعلها مقاومة للزلازل خلال العقدين الماضيين. لكن إنحفاض التسارع و حركة القاعدة للأنظمة العازلة للقواعد لم تـأخذ حقها من الدراسة. هذا العمل يستخدم نموذج محافظ جديد للدعامات المطاطية العازلة للقواعد و التي تتبنى اسلوب تصحيح المتغيرات الإنشائية خلال الزمن الحقيقي.

لتحقيق ذلك, تم القيام بتحليل و عمل نماذج باستخدام طريقة العناصر المحدودة لعمل دراسة و مقارنة بين هياكل إنشائية مثبتة القواعد و أخرى مشابهة لها و لكن معزولة القواعد باستخدام الدعامات المطاطية. حيث تم تعريض المباني لهزة أرضية (إل- سنترو) الشمالية – الجنوبية لإضافة التأثيرات اللاخطية. النموذج المستخدم للمادة شديدة الممطولية و تم ربطه لبرنامج (آباكس) كمادة معرفة للمستخدم. التوصيلات المختارة هي نوع خاص من مكتبة (آباكس) حيث تقوم بربط الدعامات المطاطية للهيكل الإنشائي و القواعد للوصول إلى الدرجة المطلوبة من تقييد الحركة.

تم التحقق من النموذج عن طريق عمل دراسة مقارنة بين النتائج المستخلصة من تحليل النموذج المقترح للمادة و النتائج المستخلصة من استخدام نماذج من استخدام تماذج (آباكس) للمواد (نموذج أوجدن للمواد). تظهر النتائج فعالية شديدة عند استخدام العزل بالدعمات المطاطية لفصل المبنى عن الحركات الإهتزازية الأرضية. إضافة لذلك, تم إثبات أن النموذج المستخدم للمادة أكثر فعالية للإمساك و التحكم بتصرف المنشأت و ذلك عن طريق ملاحظة النقص الواضح في التسارع و الزيادة في مقاومة المبنى لتأثير الهزات الأرضية.